Computers in Biology and Medicine 189 (2025) 109970

Contents lists available at ScienceDirect

Computers in Biology and Medicine

journal homepage: www.elsevier.com/locate/compbiomed

Revolutionizing biological digital twins: Integrating internet of bio-nano things, convolutional neural networks, and federated learning

Mohammad (Behdad) Jamshidi [a,*], Dinh Thai Hoang [a], Diep N. Nguyen [a], Dusit Niyato [b], Majid Ebrahimi Warkiani [c]

[a] School of Electrical and Data Engineering, University of Technology Sydney, 15 Broadway, Sydney, 2007, NSW, Australia
[b] College of Computing and Data Science, Nanyang Technological University, 50 Nanyang Ave, Block N 4, Singapore, 639798, Singapore
[c] School of Biomedical Engineering, University of Technology Sydney, 15 Broadway, Sydney, 2007, NSW, Australia

ARTICLE INFO

Keywords:
Biotechnology
Computer vision
Artificial neural networks
Convolutional neural networks (CNN)
Digital twins
Decentralized computing
Deep learning
Federated learning
Internet of Bio-Nano Things (IoBNT)

ABSTRACT

Digital twins (DTs) are advancing biotechnology by providing digital models for drug discovery, digital health applications, and biological assets, including microorganisms. However, the hypothesis posits that implementing micro- and nanoscale DTs, especially for biological entities like bacteria, presents substantial challenges. These challenges stem from the complexities of data extraction, transmission, and computation, along with the necessity for a specialized Internet of Things (IoT) infrastructure. To address these challenges, this article proposes a novel framework that leverages bio-network technologies, including the Internet of Bio-Nano Things (IoBNT), and decentralized deep learning algorithms such as federated learning (FL) and convolutional neural networks (CNN). The methodology involves using CNNs for robust pattern recognition and FL to reduce bandwidth consumption while enhancing security. IoBNT devices are utilized for precise microscopic data acquisition and transmission, which ensures minimal error rates. The results demonstrate a multi-class classification accuracy of 98.7% across 33 bacteria categories, achieving over 99% bandwidth savings. Additionally, IoBNT integration reduces biological data transfer errors by up to 98%, even under worst-case conditions. This framework is further supported by an adaptable, user-friendly dashboard, expanding its applicability across pharmaceutical and biotechnology industries.

1. Introduction

In biotechnological cyber–physical systems, Digital Twins (DTs) serve as digital representations of objects, assets, humans, and living organisms, enabling the precise creation of immersive models for bio-processes, medical systems, microorganisms, organs, and even entire humans [1–5]. Hence, to make such DTs more reliable and real-time, a wide array of components, including processors, sensors, and Internet of Things (IoT) within laboratories, hospitals, clinics, and pharmaceutical industries, are utilized [6]. An advanced version of a DT in biotechnology and medical science surpasses a simulation of diseases, patients, biological assets, and organs [7]. Thus, DTs effectively facilitate the analysis, monitoring, and adaptation of the lifecycle of microscopic creatures, biological entities, and equipment assets [8–10]. It becomes a nuanced digital, dynamic, highly detailed counterpart of living and physical biological assets, extracting data from their interactions with the environment [4]. Accordingly, DTs represent a perfect blend of the digital and physical worlds in biotechnology. They go beyond the traditional IoT model, which is limited by restricted connectivity and one-way data transfer from the physical to the virtual world [9]. Looking ahead, industrial DTs will be a significant factor in fostering the expansion of virtual environments like the Metaverse with numerous applications, including digital healthcare [10], drug development [11], and digital biotechnology [12].

Developing quick and dependable DTs in biotechnology presents significant challenges [7]. Meanwhile, the primary issue arises from the inherent variability and complexity of biological assets [13], which are unpredictable and intricate compared to engineered systems [14,15]. As a result, this complexity makes accurate modeling significantly more difficult and unreliable [16]. Another critical issue is maintaining security and privacy of biological data, particularly human-related data, which is sensitive and voluminous [17,18]. Therefore, safeguarding this data while keeping it accessible for digitalization is a major challenge [19]. Additionally, the necessity for real-time data processing in biological systems demands that digitization operates with high efficiency [20]. For this reason, the intricate nature of biological data complicates instantaneous processing and reaction, essential for the

* Corresponding author.
E-mail address: Mohammad.jamshidi@student.uts.edu.au (M. Jamshidi).

https://doi.org/10.1016/j.compbiomed.2025.109970
Received 15 August 2024; Received in revised form 28 February 2025; Accepted 1 March 2025
Available online 17 March 2025

effective functioning of DTs. Furthermore, integrating diverse biological data, ranging from organismal to molecular levels, remains a significant obstacle [16,21]. Moreover, transmission errors represent a critical challenge in data communication, which is quantified by the error rate that measures the frequency of errors occurring during data transfer. Furthermore, elevated error rates can result in substantial data loss and diminished system reliability, particularly in the context of biological data transfer, where precision and accuracy are of utmost importance [22].

The Internet of Bio-Nano Things (IoBNT) is an advanced IoT technology specifically developed to address the challenges of measurement and communication in biological assets [17,23,24]. IoBNT integrates nanoscale biological devices with communication networks, which facilitates accurate monitoring and control of biological systems. Therefore, this integration facilitates advanced applications in medical diagnostics, environmental monitoring, and biomanufacturing, ensuring more accurate, efficient, and reliable biotechnological processes. Furthermore, the specifications of IoBNT offer a powerful solution for synchronizing and effectively analyzing diverse data sets. As a result, this ability is crucial for the precise and effective use of DT in biotechnology, enabling smooth integration and real-time data processing. In addition, IoBNT provides the infrastructure needed to handle the complexity of biological data, facilitating sophisticated data analysis and interpretation. Thus, by leveraging IoBNT technology, researchers can precisely monitor and control biological systems, leading to more reliable and efficient biotechnological processes. Therefore, the existing challenges faced by DT-enabled biological systems and assets are expected to be addressed and potentially overcome by the integration of IoBNT [25].

Additionally, an important advantage of using IoBNT is its ability to optimize error rates. IoT systems, utilizing conventional wireless communication technologies such as Wi-Fi (*IEEE 802.11*) and cellular networks, typically suffer from Bit Error Rate (BER) ranging from 1% to 5% [26]. These error rates lead to substantial data losses when transferring large datasets. The errors are primarily due to packet loss, signal degradation, and interference, especially in high-noise environments, as indicated by *IEEE 802.15.4* standards for low-rate wireless personal area networks [27]. In contrast, IoBNT is specifically designed for bio-nano scale data communication, following the *IEEE P1906.1* standards for nanoscale and molecular communication frameworks, which aim to minimize BER and enhance data reliability. IoBNT demonstrates significantly lower BER, ranging from 0.01% to 0.1% [22]. However, incorporating DTs-based biological applications within IoBNT introduces its unique challenges, especially concerning sensor allocation at the nanoscale [24]. Meanwhile, the complexity and diversity of the data necessitate advanced analytical capabilities [8,28]. AI methods offer solutions for DT-based biological applications within IoBNT, which address challenges in pattern recognition and computer vision and manage the complexity and diversity of the data [29,30]. However, applying these methods demands high bandwidth to support services in laboratories and hospitals. Increased bandwidth use in biotechnology puts pressure on networks, slows data processing, and raises costs, reducing efficiency and scalability.

Thus, a robust solution to these issues is to integrate Convolutional Neural Networks (CNNs) with Federated Learning (FL) frameworks [31,32], enabling efficient analysis and processing. Integrating CNNs with FL results in a powerful algorithm for image analysis and processing. CNNs excel at identifying spatial hierarchies in images, making them ideal for tasks like image classification, segmentation, and object detection. At the same time, FL allows for decentralized training across devices, maintaining data privacy and minimizing data transfer [33,34]. In addition, this synergy leverages the image processing capabilities of CNNs [35] and the privacy-preserving and scalable features of FL [36]. Simultaneously, FL enables models to learn from diverse datasets without centralizing data, improving generalization and minimizing data breach risks. It also optimizes bandwidth usage and computational efficiency by processing data locally on edge devices. Therefore, integrating IoBNT with CNNs and FL can significantly enhance biological DTs' capabilities. IoBNT involves nanoscale biological devices connected through communication networks, enabling precise data collection from biological systems. Hence, when combined with CNNs and FL, IoBNT facilitates real-time monitoring and control of biological assets, and this integration enables continuous and accurate data collection, which CNNs process efficiently. Additionally, FL ensures effective data utilization across devices without compromising privacy, enhancing scalability and security. Together, these technologies significantly advance biological DTs, offering new possibilities in medical diagnostics, environmental monitoring, and biomanufacturing.

This study introduces an innovative framework that incorporates DT technology with IoBNT, specifically designed for applications in the biotechnology industry. This framework bridges the gap between DTs and IoBNT by incorporating advanced deep learning techniques. The system enables laboratories and hospitals (clients) to collaboratively process biological data in real time, improving data security, privacy, and accuracy without relying on central data storage. The approach also reduces complexities in creating DTs at micro and nano scales, especially for bacterial modeling, and achieves substantial bandwidth savings while providing a user-friendly dashboard for monitoring biological processes. Accordingly, IoBNT devices, specifically sensors, handle data extraction and transmission, collecting information and sending it to each client's local server within the FL framework. Thus, this approach not only addresses integration challenges but also has the potential to transform the biotechnology industry. Moreover, this framework offers essential features for extracting, transferring, preparing, and processing biological data to build reliable and real-time DT in biotechnology.

The hypothesis evaluated in this study posits that the integration of IoBNT with CNN and FL enhances the performance of DTs for biological assets at micro and nano scales. This innovative approach addresses critical challenges associated with biological data transmission, error reduction, and bandwidth optimization. The proposed framework improves data fidelity, security, and real-time processing capabilities, thereby providing a reliable and highly efficient approach for biotechnology applications. In summary, the most significant contributions and features of the proposed framework are as follows:

- The framework provides a unified and seamless aggregation, easing data security and privacy management.
- IoBNT can drastically reduces the error rates in biological data transfer, achieving up to 98% improvement.
- It uniquely reduces the complexities of micro and nano-scale DTs in biotech, especially for bacterial modeling.
- The proposed CNN-FL algorithm extracts critical insights from raw image data, achieving 98.5% accuracy.
- It achieves over 99% bandwidth savings by using FL to avoid central server dataset transfers.
- It features a user-friendly web-based dashboard for users to monitor DTs of bacteria and microorganisms.

The structure of the paper is as follows: Section 2 provides a comprehensive description of the proposed framework's architecture, which is organized into four key components: physical twins, IoBNTs, CNN integrated with FL, and a DT dashboard. In Section 3, we present the performance metrics and evaluations conducted using established benchmarks. Section 4 delves into a thorough analysis of the findings, highlighting their broader significance. Finally, Section 5, encapsulates the main contributions of the work and suggests directions for future research.

2. Related works

2.1. Introduction to DTs in biotechnology

In biopharma, DTs have encountered limitations stemming from low signal-to-noise ratios in biological systems, which complicate mathematical modeling and development pathways. This stands in contrast to other industries where DTs are more mature and widely established [37]. A study on DTs in biotechnology highlighted the benefits of process modeling, supporting workflows from development to manufacturing across diverse feedstocks, enabling efficient, cost-effective digitalization. By integrating Quality-by-Design principles, the study showcased predictive and financial benefits for consistent process modeling in biopharmaceutical applications [37]. Research has also focused on developing bioprocess DTs for mammalian cell cultures to enhance biomanufacturing efficiency [38]. This integration of in-line data collection and machine learning provided improved operational strategies and decision-making capabilities. However, limitations such as insufficient real-time data for model accuracy, complex cellular dynamics, and high regulatory compliance barriers were significant challenges [38].

The application of process analytical technology (PAT) as a key enabler for DTs in continuous biomanufacturing has been investigated [39]. By integrating real-time data and predictive models, DTs optimized process control and quality in biologics production. The benefits of PAT-driven DTs included consistent product quality, reduced costs, and improved scalability through advanced analytics and automation. Challenges included data acquisition, model accuracy, and the integration of PAT with existing processes due to high variability in bioprocesses and the need for continuous, precise measurements [39]. A flexible DT framework tailored for the biomanufacturing of advanced therapeutic medicinal products (ATMPs) was developed, focusing on CAR T cell therapy [40]. This framework facilitated the digitalization, monitoring, and management of complex production processes by integrating both manual and automated operations. The challenges involved managing high process complexity, ensuring regulatory compliance, and integrating manual tasks with automation, as well as addressing the variability of patient-specific therapies, which posed significant difficulties for standardization and consistent data acquisition [40].

Hybrid modeling approaches in DTs have also been explored to optimize complex biomanufacturing processes [41]. By combining data-driven and mechanistic approaches, these models enhanced process understanding, control, and prediction, thereby improving decision-making and operational efficiency. Hybrid DTs effectively managed process variability and uncertainty. Challenges included integrating diverse data sources, handling process variability, and establishing standardized protocols. Limited real-time data and complex regulatory requirements further hindered the effective implementation of DTs in biopharma [41]. In medicine, DTs have been leveraged for control and optimization in various applications such as diabetes management and anesthesia [42]. These virtual models of biological systems, utilizing real-time data and AI, improve personalized therapies, biomedical design, and drug delivery. DT support preclinical and clinical research, enabling better predictions and customized healthcare solutions. However, limitations included challenges in data integration, real-time monitoring, and synchronization of physical and digital models [42]. Despite the promising potential of DTs in biotechnology, several challenges must be overcome to unlock their full capabilities. The inherent complexity of biological systems, marked by high variability and low signal-to-noise ratios, presents significant barriers to achieving accurate modeling and real-time data acquisition. Advancing the future of DTs in biotechnology will likely require the development of more sophisticated hybrid modeling techniques capable of addressing the intricate nature of biological systems. Effective integration of DT in biotechnology requires adaptable frameworks that evolve with technological progress and regulatory updates.

2.2. Challenges in implementing micro and nano-scale DTs

The implementation of micro and nano-scale DTs presents numerous challenges, primarily due to the complexities of capturing accurate real-time data and integrating it effectively. At these scales, biological systems exhibit high variability and complex interactions, which significantly complicate the development and validation of robust DT models. This variability, combined with the unpredictable nature of biological processes, leads to difficulties in ensuring the accuracy and consistency of DTs, unlike in larger-scale applications where such challenges are more manageable [43]. Moreover, achieving the requisite precision in data acquisition for micro- and nano-scale DTs remains a significant challenge. Researchers frequently face obstacles in replicating the intricate conditions essential for these systems, where even slight variations can result in substantial discrepancies between the digital and physical twins. As a result, this imprecision diminishes the fidelity of DTs, thereby compromising their efficacy in biotechnology applications [44]. Additionally, the absence of standardized protocols for data collection and processing at these scales further complicates matters, as it prevents the establishment of consistent methodologies across different studies and use cases [44].

In particular, the modeling of particle breakage mechanics illustrates these challenges vividly. Studies have demonstrated that replicating the complex interactions and conditions at nano and micro scales is exceedingly difficult, often resulting in significant discrepancies between simulated behaviors and real-world outcomes [45]. Furthermore, the significant computational demands necessary to model these intricate processes introduce another layer of complexity, which renders the validation and implementation of these DTs exceedingly resource-intensive. The variability in material properties at these scales further compounds the challenge, as it heightens the difficulty of constructing accurate predictive models. Consequently, the development of flexible and adaptive modeling approaches capable of addressing these variabilities is imperative for advancing DT applications in this domain [45]. In addition, biomanufacturing has encountered its own unique challenges in implementing DTs at the micro and nano scales. The inherent complexity of biological systems, combined with the variability of process parameters, renders high-fidelity DT development particularly demanding. This is further exacerbated by the absence of real-time data integration, which is essential for accurate modeling and control. Moreover, the lack of adaptable frameworks capable of accommodating different scales and systems has created significant barriers to achieving reproducibility and robust operation in biomanufacturing processes [25]. For instance, the integration of multiscale information, necessary for developing precise predictive models, is hampered by the need for significant computational resources and standardized validation protocols [25].

To address some of these challenges, IoBNT has been proposed as a transformative framework for the digitalization and automation of biotechnology. IoBNT enables real-time monitoring and precise control at the molecular level, which is particularly advantageous for advancing the capabilities of DTs in micro and nano-scale applications [46]. By integrating nano-sensors and actuators within biological environments, IoBNT facilitates seamless communication through biological channels, such as blood vessels, allowing for innovative applications in early disease detection and personalized medicine. Nevertheless, integrating IoBNT with existing systems comes with new challenges. Ensuring precise molecular communication between devices is complex and can be significantly affected by environmental factors like temperature and pH, which disrupt communication efficiency and data reliability [47]. These disruptions pose significant challenges for the effective functioning of DTs, as consistent and accurate data are critical for maintaining the integrity of these models. Therefore, developing new security protocols that can protect biological data without compromising the functionality of IoBNT systems is essential for their broader adoption [47]. Addressing these concerns is crucial, as failure to do so

could hinder the integration of IoBNT into DT frameworks and limit their potential benefits in healthcare and biomanufacturing.

Despite these hurdles, the potential advantages of incorporating IoBNT into micro and nano-scale DTs remain substantial. Moreover, IoBNT has the potential to enable advanced biomedical applications, such as targeted drug delivery and automated therapeutic interventions, which surpass the capabilities of traditional DTs [48]. However, to maximize these benefits, significant advancements in biocyber interfaces and the seamless integration of IoBNT with existing digital networks are needed. Achieving this integration is critical for enabling the real-time data processing and automation necessary for effective DT deployment in biotechnology [48]. Looking ahead, the future of DTs in micro and nano-scale applications will likely depend on the continued development of IoBNT frameworks that can overcome current limitations in data acquisition, integration, and security. Additionally, interdisciplinary collaboration between biologists, engineers, and data scientists will be essential for tackling the complex challenges associated with modeling and controlling biological systems at these scales [49]. By creating more advanced and flexible frameworks, the capabilities of DTs can be expanded beyond their existing boundaries. Ultimately, addressing the challenges associated with implementing micro and nano-scale DTs is essential for unlocking the complete potential of these technologies in revolutionizing the biotechnology industry.

2.3. Combinations of FL with CNN and FL with DTs

Recent advancements in ML methods have significantly impacted e-health and biotechnology, offering powerful tools for data analysis, diagnosis, and treatment optimization [50]. Approaches like artificial neural networks (ANNs) have been enhanced by hybrid algorithms, such as invasive weed optimization combined with differential evolutionary models, improving the accuracy and efficiency of training [51]. Deep learning techniques, including CNN and LSTM ensembles, are also enabling more sophisticated image captioning for medical imaging [52]. These innovations are further supported by mixed analog–digital infrastructure, fostering better classification in biomedical systems. Together, these advancements are shaping the future of e-health and biotechnology [53].

The combination of FL with DTs and CNNs has been recognized as a promising strategy to address concerns regarding data privacy and to improve model performance across various applications. However, despite its significant potential, the deployment of these integrated frameworks encounters numerous challenges, which include computational complexity and communication overhead [12]. This subsection explores related works on the combination of FL with DTs and FL with CNNs across different domains, highlighting both the opportunities and limitations of these methods. In the healthcare sector, the combination of FL and CNNs has been widely applied for secure medical image analysis. One study focused on using FL to train CNN models on distributed MRI data for brain tumor detection, preserving patient privacy without the need for data centralization [54]. Local CNN models were independently trained at each medical institution, and their weights were combined using FL. This approach achieved a classification accuracy of 91.05%, which was marginally lower than that of traditional centralized models. The main challenges highlighted included the computational complexity of training CNNs on large-scale datasets and the communication overhead associated with aggregating model parameters. Moreover, ensuring consistent model performance across diverse local datasets with varying quality and characteristics proved challenging, underscoring the limitations of FL [54].

Expanding on this concept, researchers developed a framework that integrated FL with CNN-LSTM models for Autism Spectrum Disorder (ASD) detection [55]. This system processed multimodal datasets from various clinical laboratories, utilizing FL to aggregate results securely for optimized ASD prediction. The combined use of CNNs for feature extraction and LSTM models for temporal sequence learning enabled accurate detection of ASD, achieving around 99% accuracy. However, the framework faced scalability issues, particularly in resource-constrained environments. Furthermore, the inability to update models in real-time hindered the framework's effectiveness in supporting dynamic patient treatments, illustrating the need for more efficient integration strategies to enhance the performance and scalability of FL-based systems [55]. In another study, FL was combined with transfer learning techniques to classify breast cancer images while preserving data privacy [56]. By utilizing multiple local environments, the researchers were able to train CNN models without sharing sensitive patient data. This decentralized methodology enabled effective feature extraction and classification through the use of FeAvg-CNN and MobileNet models, which demonstrated high accuracy and recall rates. Despite these achievements, the study identified several challenges, including communication overheads that impacted the overall model performance. The decentralized structure of FL posed difficulties in maintaining consistent accuracy across diverse datasets, particularly when data distributions varied significantly among different local environments. Additionally, the resource-intensive nature of FL, combined with the requirement for frequent communication between local nodes and the central server, presented substantial barriers to its broader adoption in resource-constrained healthcare settings [56].

Within the framework of the Industrial Internet of Things (IIoT), FL has been applied to improve the integration of DTs by enabling distributed learning without data centralization [57]. This method improved model accuracy and decision-making by enabling DT to learn from decentralized data sources in real time. Despite these advantages, the study identified several challenges, including limited communication bandwidth and high computational demands. However, synchronizing DTs with real-world conditions and ensuring data integrity remained significant obstacles, limiting the framework's efficiency in dynamic industrial environments [57]. These results suggest that further research is needed to develop better communication protocols and synchronization methods for integrating FL with DT in IIoT applications. In 6G-enabled Industrial IoT environments, FL was incorporated with DTs to support efficient and secure data processing within Digital Twin Wireless Networks (DTWN) [58]. The inclusion of blockchain technology ensured data integrity and privacy while optimizing edge computing resources. Nevertheless, the study faced challenges related to high communication costs, limited bandwidth, and dynamic network conditions. Managing resource allocation and latency remained critical concerns, as maintaining synchronization between DTs and their physical counterparts was essential for effective operation in complex IoT scenarios) [58]. This highlights the need for advanced resource management and scheduling strategies to improve the integration of FL and DTs in such environments.

Furthermore, a study explored the use of FL in Industrial IoT to address challenges related to data privacy and communication efficiency in DTs [57]. The researchers applied an asynchronous FL scheme combined with deep reinforcement learning to manage aggregation frequency and clustering. This approach exhibited superior performance with respect to convergence and energy savings when compared to traditional methods. However, addressing the computational and communication overheads associated with FL remained challenging, particularly in maintaining consistent model updates across diverse devices. Privacy concerns arising from decentralized data sources also presented significant obstacles to the adoption of FL in industrial settings. The study highlighted the necessity for developing more robust and efficient FL algorithms capable of meeting the unique requirements of Industrial IoT environments [57].

Overall, while the integration of FL with DTs and CNNs provides promising solutions for improving data privacy and model performance across various applications, numerous challenges persist. The complexity associated with managing communication overhead and addressing computational demands must be resolved to fully exploit the potential of these frameworks. Future research should concentrate on the development of adaptive learning strategies, efficient resource

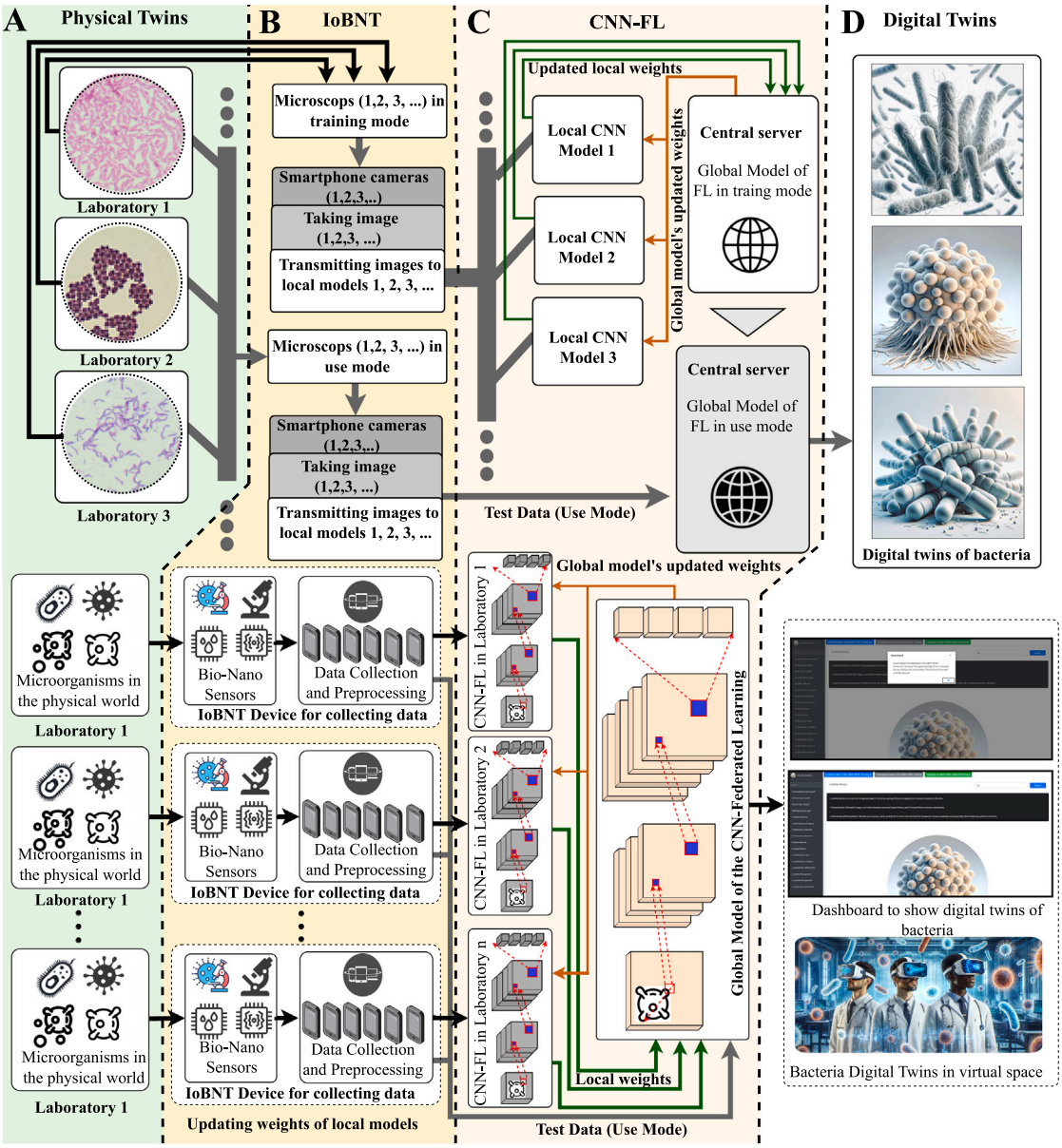

Fig. 1. The proposed framework for creating bacterial DTs using CNN, FL, and IoBNT technology; A: Real bacteria samples are observed and analyzed under a microscope, representing the physical counterparts of the DTs; B: IoBNT devices capture microscopic images of bacteria and transmit this data to local CNN models for initial processing and analysis; C: The FL framework collects and combines the weights from multiple local CNN models, creating a robust global model without sharing raw data, thus preserving privacy; D: An intuitive dashboard enables users to observe and interact with the DTs of bacteria in real time, accessible via a monitor or VR headset through an online HTML interface.

management techniques, and scalable frameworks capable of accommodating the diverse requirements of various domains. By overcoming these challenges, the integration of FL, DTs, and CNNs can unlock unprecedented opportunities for secure and efficient data processing in healthcare, smart cities, and industrial environments.

3. Materials and methods

Fig. 1 illustrates the architecture of this framework, which consists of four sections: physical twins, IoBNTs, CNN-FL, and the DT dashboard. A physical twin is the actual asset, human, object, creature, or any entity that serves as the real-world counterpart for creating its corresponding DT [59,60]. In this work, the term physical twins specifically refers to the actual bacteria being studied to evaluate the framework. Moreover, Fig. 1A clearly depicts the physical presence of bacteria in laboratories and hospitals, showcasing real-world samples.

As we explore the framework in greater detail, Fig. 1B emphasizes the role of IoBNT in facilitating efficient data extraction and transmission. Additionally, the integration of CNN-FL within the framework is illustrated in Fig. 1C, showcasing its functionality in data processing and analysis. Finally, Fig. 1D depicts a user-friendly dashboard that visualizes DTs for users, accessible through a web interface or VR headset. The proposed framework seeks to address the limitations of integrating DTs with IoBNT in biological systems by employing advanced deep learning algorithms, such as FL and CNN. Notably, in Fig. 1C, the client represents laboratories participating in the FL network, which include entities like organizations engaged in the collaborative learning process of the FL algorithm [32]. Furthermore, IoBNT specifically refers to sensors responsible for data extraction and transmission, which collect data and transmit it to the local server of each client within the FL framework.

Building on the framework's components, the setup for CNNs involves configuring them to achieve precise pattern recognition and

advanced image processing, which is crucial for modeling bacterial images within DTs. Moreover, FL is applied across a network of IoBNT devices with CNN capabilities, allowing localized data processing on each device. This approach boosts privacy and reduces the need for data transfer. For evaluation, 10% of the dataset is allocated for testing and 90% for training, with both CNN-FL and CNN models using identical datasets. In the CNN-FL framework, the training data is evenly distributed among three clients, while the test data assesses the global model's performance [61]. Moreover, the CNN-FL model trains for 100 rounds. A custom-trained CNN is developed from the ground up to match the unique attributes of our dataset. As a result, data collected from various IoBNT devices enhances the CNN models, improving their precision in detecting bacterial activity. This fusion of CNN-FL with IoBNT seamlessly combines nanoscale biological data interpretation with distributed data processing, achieving unprecedented precision and robustness.

3.1. DTs in biotechnology

DTs, which are sophisticated virtual counterparts of physical entities or systems, simulate real-time behaviors [9]. In biotechnology and biomanufacturing, DTs are extensively used for the design, optimization, monitoring, and control of bioprocesses and bioproducts [62–64]. To create effective DTs for biotechnological applications, a systematic methodology that integrates both data-driven and model-driven approaches is proposed. These methodologies enable the accurate simulation of complex biological systems, thereby enhancing the optimization of processes for producing biomaterials, drugs, and vaccines. Initially, the development of DTs begins with high-quality data collection, which is subsequently utilized to construct detailed models representing the target bioprocesses or bioproducts [65]. Subsequently, iterative testing in virtual environments validates and refines these models, ensuring reliable replication of physical behaviors. This process not only accelerates deployment but also reduces the time-to-market for new bioproducts [1–3]. Furthermore, DTs facilitate the simulation of diverse scenarios, enabling the optimization of processes within a controlled digital environment. For instance, DTs can model drug interactions with biological systems, providing predictions of outcomes and optimizing formulations without the need for extensive experimental trials. They are also instrumental in simulating disease progression and treatment responses, advancing the development of personalized medicine. In the domain of biomanufacturing, DTs enhance biological process optimization, ensuring both quality and efficiency. Moreover, DTs are employed to model ecosystems and microbiomes, predicting their responses to environmental changes. Similarly, they simulate plant and animal growth in agricultural applications, aiming to optimize yields and the efficient use of resources. Consequently, this methodology accelerates development cycles and enhances product precision and reliability by identifying potential issues and evaluating solutions without the necessity of physical trials.

In the biopharmaceutical sector, DTs play a crucial role in optimizing cell fermentation processes and managing supply chains, providing a platform for precise modifications to enhance efficiency and foster innovation [62]. Additionally, DTs incorporate data from physical environments, facilitating uninterrupted observation and adaptive control, which allow processes to be fine-tuned for optimal performance. Nevertheless, the management and analysis of large datasets, alongside the development of complex models, demand significant computational resources and specialized expertise, both of which are vital for ensuring the effectiveness of DTs in biotechnology. Finally, maintaining the reliability and accuracy of models is imperative, as these models must consistently adapt to and accurately predict the behavior of the physical entities they represent.

3.2. Optimizing DT performance

Optimizing DT performance involves real-time monitoring, data processing, and model refinement [9,63]. To achieve this, a robust infrastructure with high-resolution sensors and data acquisition systems is essential for the continuous collection of data on bioprocesses and bioproducts [65]. Furthermore, advanced computational systems are required to process these vast data streams to extract actionable insights, which are crucial for timely anomaly detection and maintaining process stability [1]. Therefore, it is imperative to utilize high-performance computing and sophisticated algorithms for real-time data analysis. Moreover, AI techniques play a pivotal role in processing and interpreting data, thereby optimizing bioprocesses and predicting outcomes. To replicate biological entities under various conditions, it is necessary to develop dynamic models. Consequently, iterative testing and refinement are essential to ensure accurate predictions, identifying potential issues before they affect actual processes. By integrating CNNs with FL and IoBNT, we can significantly enhance DT capabilities. Specifically, CNN-FL enables decentralized learning for continuous model updates [61], while IoBNT ensures real-time interaction between digital and physical domains, thereby improving model accuracy.

Additionally, continuously updating DT models with real-time data and feedback is crucial. Regularly refining models with new data improves efficiency, safety, and consistency. In our framework, these technologies are utilized to enhance DT performance, including precise real-time data extraction, effective deep learning model training for biological data, optimized bandwidth usage for data transmission between physical twins and DT, and addressing security and privacy challenges.

3.3. CNN-FL integration

CNNs are a class of deep neural networks known for their efficacy in visual imagery analysis [15]. CNNs automate feature extraction, which enhances efficiency and accuracy in identifying and extracting patterns from data. They have revolutionized fields such as image classification and object detection, playing a pivotal role in the advancement of AI.

A typical CNN structure comprises the following components:

1. Convolutional Layer: This layer applies convolutional operations to the input data to generate feature maps.

$$\mathbf{O}_{ij}^{k} = \sum_{m=1}^{M}\sum_{n=1}^{N} \mathbf{I}_{(i+m-1)(j+n-1)} \cdot \mathbf{K}_{mn}^{k} + b^{k}, \tag{1}$$

where $\mathbf{O}_{ij}^{k}$ is the output feature map at position (i, j) for the kth filter, $\mathbf{I}$ represents the input image, $\mathbf{K}^{k}$ denotes the kth convolution kernel (a filter that slides over the input image), and b^{k} is the bias term added to the convolution result.

Eq. (1) performs the convolution operation, which involves element-wise multiplication of the input image patch with the filter, summing the results, and adding a bias term.

2. Activation Function: The activation function, typically the Rectified Linear Unit (ReLU), is applied element-wise to introduce non-linearity into the model.

$$\mathbf{A}_{ij}^{k} = \max(0, \mathbf{O}_{ij}^{k}), \tag{2}$$

where $\mathbf{A}_{ij}^{k}$ is the activation output at position (i, j) for the kth filter.

The ReLU activation function outputs the input directly if it is positive; otherwise, it outputs zero. This helps in introducing non-linearity and allows the network to learn complex patterns.

3. Pooling Layer: Pooling layers reduce the spatial dimensions of the feature maps, which can reduce computational load and controlling overfitting. In max pooling:

$$\mathbf{P}_{ij}^{k} = \max_{(m,n)\in\mathcal{P}} \mathbf{A}_{(i+m)(j+n)}^{k}, \tag{3}$$

where $\mathbf{P}_{ij}^{k}$ is the pooled output at position (i, j) for the kth filter, and $\mathcal{P}$ is the pooling window.

Max pooling selects the maximum value from the feature map patch covered by the pooling window. This operation helps in downsampling the feature map, reducing its dimensions while retaining important features.

4. Fully Connected Layer: This layer maps the extracted features to the output classes.

$$\mathbf{z} = \mathbf{W}\mathbf{h} + \mathbf{b}, \tag{4}$$

where $\mathbf{z}$ is the output vector (e.g., class scores), $\mathbf{W}$ is the weight matrix, $\mathbf{h}$ is the flattened input feature map, and $\mathbf{b}$ is the bias vector.

The fully connected layer multiplies the flattened input feature map by the weight matrix, adds the bias vector, and outputs the result. This operation is similar to a traditional neural network layer and is used to make final predictions.

To enhance flexibility and scalability for embedded vision applications, we integrate MobileNetV2 [66] into our framework. MobileNetV2 is designed for efficient image classification on mobile and embedded vision applications, leveraging inverted residuals and linear bottlenecks. FL is a cutting-edge approach to machine learning that enables multiple participants, referred to as clients or workers, to collaboratively train a model while keeping their data decentralized and private [31,32]. This technique contrasts with traditional centralized CNN methods where data is pooled into a single location [61]. In FL, each participant trains its model based on its local data and shares model updates, not the data itself, with a global server. The server consolidates these updates to enhance the overall model, preserving privacy and security while leveraging distributed data sources.

The CNN-FL integration involves the following steps:

1. Local Model Training: Each client i trains its local model $\mathbf{w}_i$ using its own data $\mathcal{D}_i$. The local update rule is

$$\mathbf{w}_i^{(t+1)} = \mathbf{w}_i^{(t)} - \eta \nabla \mathcal{L}_i(\mathbf{w}_i^{(t)}; \mathcal{D}_i), \tag{5}$$

where $\mathbf{w}_i^{(t+1)}$ is the updated local model weights at iteration $t+1$, $\mathbf{w}_i^{(t)}$ is the local model weights at iteration t, η is the learning rate, and $\nabla \mathcal{L}_i(\mathbf{w}_i^{(t)}; \mathcal{D}_i)$ is the gradient of the local loss function $\mathcal{L}_i$ with respect to the model weights, computed using the local data $\mathcal{D}_i$.

This equation updates the local model weights by taking a step in the direction of the negative gradient of the loss function, scaled by the learning rate.

2. Global Model Aggregation: The central server aggregates the local models from all clients to update the global model $\mathbf{w}$:

$$\mathbf{w}^{(t+1)} = \sum_{i=1}^{N} \frac{n_i}{n} \mathbf{w}_i^{(t+1)}, \tag{6}$$

where $\mathbf{w}^{(t+1)}$ is the updated global model weights at iteration $t+1$, N is the total number of clients, and n_i is the number of data samples on client i. $n = \sum_{i=1}^{N} n_i$ is the total number of data samples across all clients, and $\mathbf{w}_i^{(t+1)}$ is the updated local model weights for client i at iteration $t+1$.

The expression in (6) performs a weighted averaging of the local model weights, where the weight for each client is proportional to the number of data points it holds.

3. Federated Averaging (FedAvg): The Federated Averaging algorithm aggregates the local model updates using weighted averaging:

$$\mathbf{w}^{(t+1)} = \mathbf{w}^{(t)} - \eta \sum_{i=1}^{N} \frac{n_i}{n} \left(\mathbf{w}_i^{(t+1)} - \mathbf{w}^{(t)} \right). \tag{7}$$

This equation adjusts the global model weights based on the weighted difference between the local model updates and the current global model weights.

When CNNs are integrated with FL, they leverage the power of CNNs to process and learn from image data in a privacy-preserving manner across distributed datasets [61]. This combination is particularly powerful for applications where data privacy is paramount and where training data is naturally distributed across multiple locations, such as in medical imaging analysis across different hospitals. The proposed CNN-FL algorithm is represented as follows:

1. Local Model Update: Each client i trains a local CNN model $\mathbf{w}_i^{(t+1)}$ using its own subset of data. The local loss function $\mathcal{L}_i$ is typically a cross-entropy loss for classification tasks [67]:

$$\mathcal{L}_i(\mathbf{w}_i) = -\frac{1}{|\mathcal{D}_i|} \sum_{(x,y)\in\mathcal{D}_i} y \log f_{\mathbf{w}_i}(x), \tag{8}$$

where $\mathcal{L}_i(\mathbf{w}_i)$ is the local loss function for client i, $|\mathcal{D}_i|$ is the size of the local dataset $\mathcal{D}_i$, x and y are the input and label, respectively, and $f_{\mathbf{w}_i}(x)$ is the prediction of the CNN with weights $\mathbf{w}_i$.

The expression in (8) calculates the cross-entropy loss, which measures the difference between the predicted probabilities and the actual labels.

2. Global Model Update: The global model $\mathbf{w}^{(t+1)}$ is updated by averaging the local models:

$$\mathbf{w}^{(t+1)} = \sum_{i=1}^{N} \frac{n_i}{n} \mathbf{w}_i^{(t+1)}. \tag{9}$$

The expression in (9) is the same as previously described, performing a weighted averaging of the local model weights to update the global model.

3. Objective Function: The overall objective function for the CNN-FL framework can be defined as the weighted sum of the local loss functions:

$$\mathcal{L}(\mathbf{w}) = \sum_{i=1}^{N} \frac{n_i}{n} \mathcal{L}_i(\mathbf{w}), \tag{10}$$

where $\mathcal{L}(\mathbf{w})$ is the overall objective function, $\mathcal{L}_i(\mathbf{w})$ is the local loss function for client i, n_i is the number of data points on client i, and $n = \sum_{i=1}^{N} n_i$ is the total number of data points across all clients.

This equation defines the overall objective as the weighted sum of the local loss functions, ensuring that each client's contribution is proportional to the size of its dataset.

4. Communication and Synchronization: After each local training epoch, clients communicate their updated models to the central server, which synchronizes the global model. This process continues iteratively until the model converges.

By integrating CNNs with FL, the framework leverages the strengths of both technologies: the powerful feature extraction capabilities of CNNs and the privacy-preserving distributed learning approach of FL. This combination is particularly effective for applications requiring secure and distributed data analysis, such as medical imaging.

3.4. Decentralized CNN training with FL implemented using flower (FLWR)

We use Flower (FLWR) with various adjustments in the proposed framework to enhance customization and adaptability in our framework [68]. Such embedded characteristics address diverse application requirements while ensuring adaptability. Flower facilitates the coordination of multiple clients, each training on a distinct portion of the dataset without necessitating centralized data storage, which ensures data privacy and adheres to distributed data policies. The clients, uniformly configured with an equal allocation of training and validation images, independently train their models using a standardized architecture. During each round, every client trains its model for one epoch and transmits the resulting model weights to a central server. The server functionality in Flower aggregates these weights through a weighted average approach, ensuring that the contribution of each client is proportional to the size of its respective dataset. This approach, along with the flexibility and scalability of Flower, enables efficient model training across distributed nodes while reducing communication overhead and ensuring data security.

3.5. Implementing IoBNT in biotechnology

IoBNT combines nanotechnology, biotechnology, and information technology to create interconnected networks of biological and nano-engineered devices [24,69]. This methodology details the systematic steps for developing and implementing IoBNT systems, which can revolutionize biotechnology applications in healthcare and environmental monitoring. The development process begins with designing and fabricating molecular sensors, actuators, and miniature computational components capable of interacting with biological systems at cellular and molecular levels [25]. Biocompatible materials ensure the seamless integration of these devices within biological environments. IoBNT devices are embedded to monitor and interact with biological entities in real-time, enabled to collect, process, and transmit biological data efficiently through advanced interfaces.

IoBNT technologies transform medical diagnostics and treatment in healthcare, providing highly personalized medical interventions. Real-time data collected from IoBNT devices fosters personalized medicine by enabling precise monitoring of patient health conditions and timely treatment adjustments [10,69]. In the realm of environmental biotechnology, IoBNT devices exhibit exceptional precision and sensitivity in identifying contaminants and microbial threats, enabling advanced strategies for environmental surveillance and sustainable management. As IoBNT technologies advance, they will enable more sophisticated integration of biological and digital systems, leading to breakthroughs in diagnostics, environmental management, and personalized healthcare [6]. This evolution promises to enhance the accuracy and responsiveness of biotechnological applications, ultimately driving innovation and improving quality of life across diverse fields.

3.6. Metrics and measurement for evaluating performance

This study utilizes a set of essential metrics – accuracy, precision, recall, and the F1-score [70] – to rigorously evaluate our classification models. These measures collectively offer an in-depth assessment of the model's capability to produce precise predictions and effectively address class imbalances.

Accuracy signifies the classifier's ability to produce correct predictions across all instances. It is calculated as the proportion of correctly classified samples to the total number of predictions made.

$$\text{Accuracy} = \frac{\text{Correctly Classified Instances}}{\text{Total Predictions}} \tag{11}$$

Precision quantifies the reliability of positive classifications, measuring the proportion of correctly identified positive cases among all instances predicted as positive, including false positives.

$$\text{Precision} = \frac{\text{True Positives}}{\text{True Positives} + \text{False Positives}} \tag{12}$$

Recall, also known as sensitivity, evaluates how effectively the classifier detects all actual positive cases. It is determined by the ratio of true positives to the total number of actual positives, considering both correctly identified cases and those mistakenly classified as negatives.

$$\text{Recall} = \frac{\text{True Positives}}{\text{True Positives} + \text{False Negatives}} \tag{13}$$

F1-score serves as a balanced metric that harmonizes precision and recall, offering a single numerical representation of the classifier's performance. This measure is particularly advantageous when dealing with imbalanced datasets, ensuring that both false positives and false negatives are fairly accounted for.

$$\text{F1-score} = 2 \times \frac{\text{Precision} \times \text{Recall}}{\text{Precision} + \text{Recall}} \tag{14}$$

By integrating precision and recall into a unified evaluation, the F1-score delivers a comprehensive insight into a model's classification effectiveness. This makes it a crucial benchmark for assessing scenarios where the consequences of false classifications must be carefully managed.

3.7. Dataset preparation

The dataset used in this study was obtained from a previously published study in Elsevier [71], ensuring its peer-reviewed validation. It comprises 2033 RGB images of bacteria collected from blood, urine, and skin samples of patients. Following pure culture, the bacteria were stained using the Gram method, and species identification was conducted by laboratory experts. The images were captured using a Nikon E200 microscope equipped with a 100x objective lens. Importantly, no data augmentation techniques were applied to this dataset to maintain its original characteristics. To avoid bias in the analysis, the number of images representing each species was balanced. The preprocessing of this dataset involved several crucial steps to ensure the images were prepared correctly for the machine learning framework. First, each image was normalized, which involved scaling the pixel values to a range between 0 and 1, making the data easier for the neural network to process. Additionally, the images were resized to a standard dimension of 224×224 pixels, ensuring consistency in input size.

Next, the normalized and resized images were paired with their corresponding labels, which represented various bacterial species, enabling the machine learning model to associate each image with its correct category. The dataset was subsequently divided into batches to facilitate efficient processing during training, validation, and testing phases. During the training process, these batches were shuffled to prevent the model from learning any specific sequence of the images. Following prediction, the batched data was unwrapped, and the predicted labels were converted from numerical values back into their respective class names, thereby enhancing the interpretability of the results. The dataset was split with 90% used for training and 10% for testing. In the FL setup, the dataset was evenly distributed among clients. Each client trained its model locally on its subset of data and sent updates to the central server. Batches were created for efficient processing, and early stopping was employed during training to avoid overfitting. After training, the model was evaluated on the independent test dataset, ensuring it was tested on unseen data for unbiased performance assessment. Table 1 provides an overview of the number of images collected for each of the 33 bacteria species used in training the proposed framework.

3.8. Experimental setting

The proposed architecture leverages MobileNetV2, a lightweight CNN, as the core model to address the unique computational constraints of IoBNT devices. This CNN backbone is initialized with weights pre-trained on ImageNet to maximize transfer learning benefits, enhancing feature extraction while reducing training time. Following the MobileNetV2 layers, a Global Average Pooling layer compresses spatial dimensions, facilitating efficient aggregation of feature maps. This pooling layer connects to a dense layer with 33 softmax-activated units, allowing for the classification of 33 distinct classes. Such a streamlined architecture ensures high accuracy in feature extraction with minimal trainable parameters, making it suitable for real-time deployment in resource-limited IoBNT environments. Each learning cycle involves localized training of CNN models on individual client devices, an essential component of FL where data remains on the device, thus enhancing data privacy and security. For training efficiency and stability, a batch size of 32 and an input resolution of 224×224 pixels are used, while a learning rate of 5×10^{-5} is carefully chosen to balance convergence speed and generalization. To mitigate overfitting, early stopping with a patience threshold of three epochs monitors validation loss trends, halting training if improvement plateaus.

After local training, updated model weights are transmitted to a central server where Federated Averaging (FedAvg) aggregates these updates. FedAvg, a weighted averaging technique, accounts for the number of data samples per client, thus allowing a more accurate and representative global model that reflects data heterogeneity across

Table 1
The number of images within each of the 33 bacteria categories.

Bacteria species	Collected data
Veillonella	58
Streptococcus agalactiae	65
Staphylococcus saprophyticus	60
Staphylococcus epidermidis	59
Staphylococcus aureus	64
Pseudomonas aeruginosa	63
Proteus	60
Propionibacterium acnes	61
Porphyromonas gingivalis	65
Neisseria gonorrhoeae	69
Micrococcus spp	63
Listeria monocytogenes	63
Lactobacillus salivarius	60
Lactobacillus rhamnosus	60
Lactobacillus reuteri	60
Lactobacillus plantarum	61
Lactobacillus paracasei	60
Lactobacillus johnsonii	61
Lactobacillus jensenii	66
Lactobacillus gasseri	61
Lactobacillus delbrueckii	59
Lactobacillus crispatus	57
Lactobacillus casei	60
Fusobacterium	62
Escherichia coli	59
Enterococcus faecium	57
Enterococcus faecalis	60
Clostridium perfringens	62
Candida albicans	62
Bifidobacterium spp	64
Bacteroides fragilis	65
Actinomyces israelii	67
Acinetobacter baumannii	60
Total	**2033**

clients. Reproducibility is crucial in FL, especially for IoBNT applications with non-deterministic edge devices. Therefore, random seeds for key libraries, including NumPy, TensorFlow, and Python's random library, are uniformly set across clients and the server, ensuring consistency in data splits, model initialization, and other stochastic processes. The local models employ the categorical cross-entropy loss function to optimize multi-class classification, combined with the Adam optimizer to balance computational efficiency and model convergence. Data handling is facilitated by TensorFlow's Dataset API, which not only manages data batching and loading but also implements techniques such as shuffling and parallel loading, thereby enhancing computational efficiency during each training cycle. For data preprocessing, images undergo normalization to standardize pixel intensity ranges, optimizing inputs for the MobileNetV2 architecture. Resizing is applied to align with the CNN's input dimensions, ensuring that each image adheres to the 224 × 224 pixel resolution required by the model. The normalization of input data not only reduces potential biases but also aligns with best practices in deep learning, where standardized input distributions improve convergence rates.

In this FL framework, the FedAvg strategy is pivotal, as it enables a decentralized yet unified model that benefits from diverse client data distributions. By averaging weights proportionally to each client's data volume, FedAvg maintains a balanced representation of heterogeneous data sources, which is particularly advantageous for IoBNT applications where each client may capture unique biological or environmental information. Consequently, the global model achieves improved generalization, leveraging insights from localized data without compromising privacy, a key consideration in medical or sensitive applications within the IoBNT ecosystem. This FL setup not only optimizes the model's performance across diverse data but also maintains privacy and data integrity, making it a robust choice for real-time IoBNT deployments.

Furthermore, to address the concern of overfitting, several techniques were implemented in our framework. First, we applied early stopping to halt training when validation accuracy plateaued, preventing the model from over-learning. Additionally, dropout layers were used for regularization, randomly deactivating neurons during training to improve generalization. We also performed cross-validation by partitioning the dataset, which ensured that the model was tested on different data subsets, enhancing its ability to generalize. Furthermore, our FL approach, where the model trains across multiple clients with varied data subsets, further helped to avoid overfitting and improve robustness to unseen data.

4. Results

4.1. Convergence rate

In a centralized CNN framework, the central server is tasked with processing the entire dataset, which leads to considerable computational bottlenecks and inefficiencies. For instance, a dataset comprising 2033 RGB images, each with a resolution of 224 × 224 pixels, corresponds to approximately 304 million pixels in total. This substantial data volume can result in delays and heightened resource consumption on the server, thereby decelerating both training and inference procedures. Centralized systems often experience latency and inefficiencies because all data must be processed centrally, which slows down updates and reduces the accuracy of real-time analysis. Furthermore, transferring the entire dataset to a central server demands significant bandwidth and poses critical privacy concerns. In such a centralized CNN configuration, the server is responsible for 100% of the data processing, further intensifying delays and aggravating computational bottlenecks.

In contrast, our framework, which incorporates CNN-FL, efficiently distributes the computational workload across multiple clients, thereby alleviating the limitations associated with centralized data processing. In a setup involving 3 clients, each client processes approximately 678 images, which significantly reduces the computational burden on a single server and facilitates more efficient processing. This decentralized methodology enables more accurate and responsive updates for DTs by integrating real-time data from multiple sources. Our proposed framework demonstrates considerable enhancements in training speed when compared to conventional centralized CNN models. The results reveal a remarkable improvement in training convergence using the CNN-FL framework, which substantially outperforms traditional centralized CNN configurations. The performance evaluation, as presented in Fig. 2, provides a detailed comparison of various configurations. Specifically, Fig. 2A illustrates an inefficient training accuracy convergence, requiring 120 rounds for the centralized CNN model to stabilize. Conversely, Fig. 2E and Fig. 2I depict a significant advancement, achieving training accuracy convergence in only 40 rounds. This substantial improvement underscores the efficacy of the proposed configurations in expediting the training process.

The CNN-FL framework with 2 and 3 clients (Fig. 2E and Fig. 2I) achieves 95% accuracy within the first 20 rounds, compared to the centralized CNN model which requires over 110 epochs to reach the same level of accuracy (Fig. 2A). Moreover, our framework attains over 98% accuracy in only 40 rounds, whereas centralized CNNs need 120 epochs for similar results. This dramatic reduction in training rounds underscores the effectiveness of our optimization strategies, enabling faster deployment and iteration of models across multiple laboratories. The efficiency gains of the CNN-FL framework are further highlighted through the analysis of convergence training graphs. The logarithmic perspective of the convergence training graph for the centralized CNN (Fig. 2B) reveals an inefficient training process, with prolonged stabilization times. In contrast, Fig. 2F and Fig. 2J illustrate the fast and efficient convergence of our CNN-FL framework. These graphs provide a clear visualization of the efficiency gains achieved through our proposed framework, demonstrating a significant reduction in the number of training rounds required to achieve high accuracy.

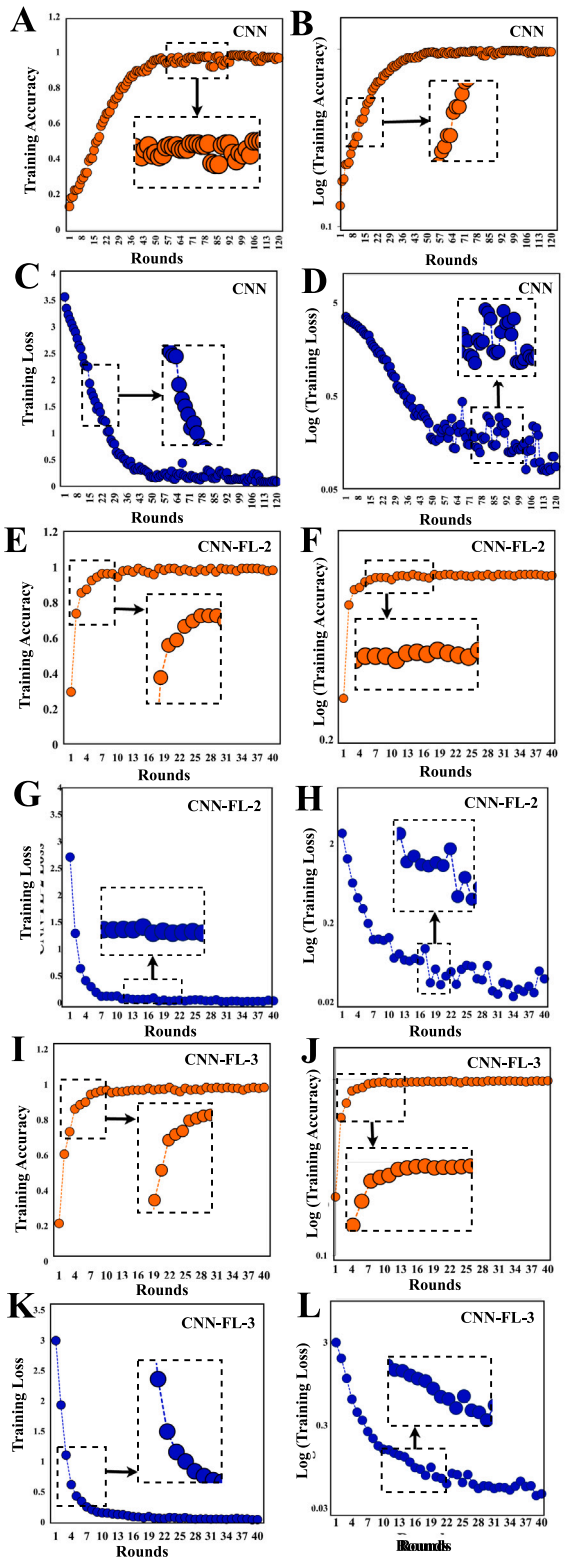

Fig. 2. Performance evaluation of the proposed CNN-FL framework (CNN-FL-2 and CNN-FL-3) compared to centralized CNN model (CNN); A: Convergence training graph (centralized CNN); B: Logarithmic convergence graph (centralized CNN); C: Loss convergence graph (centralized CNN); D: Logarithmic loss convergence graph (centralized CNN); E: Convergence training graph (CNN-F with 2 laboratories); F: Logarithmic convergence graph (CNN-F with 2 laboratories); G: Loss convergence graph (CNN-F with 2 laboratories); H: Logarithmic loss convergence graph (CNN-F with 2 laboratories); I: Convergence training graph (CNN-F with 3 laboratories); J: Logarithmic convergence graph (CNN-F with 3 laboratories); K: Loss convergence graph (CNN-F with 3 laboratories); L: Logarithmic loss convergence graph (CNN-F with 3 laboratories).

Accordingly, the convergence training graph of the loss for the traditional CNN model (Fig. 2C) exhibits slower stabilization compared to the CNN-FL framework employing 2 and 3 clients (Fig. 2G and Fig. 2K). Furthermore, the logarithmic representation of the convergence training loss graph for the centralized CNN model (Fig. 2D) and the CNN-FL framework with 2 and 3 clients (Fig. 2H and Fig. 2L) highlights the efficiency and effectiveness of the proposed approach. This detailed analysis underscores the enhanced performance of the CNN-FL framework in terms of both convergence speed and accuracy. The primary factor driving these improvements in training speed and accuracy is the decentralized nature of the framework, which distributes the computational workload across multiple clients. This distribution mitigates the bottlenecks and inefficiencies characteristic of centralized systems, where the central server is required to process the entire dataset.

By enabling each client to process a portion of the dataset, the framework significantly alleviates the computational burden on any single server, thereby accelerating convergence, as illustrated in the performance evaluation (Fig. 2). The convergence results demonstrate that the CNN-FL model attains 95% accuracy within only 20 rounds and exceeds 98% accuracy in 40 rounds, which directly results from distributing the learning process across multiple clients. This outcome is anticipated, as FL allows each client to perform training on its local data while transmitting only model updates instead of the entire dataset. This method not only preserves data privacy but also substantially reduces bandwidth requirements, as detailed in the bandwidth savings analysis (Table 2). The enhanced performance of the CNN-FL framework can further be ascribed to its ability to aggregate knowledge from multiple sources, thereby generating more generalized and robust models. By training on decentralized data, the CNN-FL model effectively mitigates overfitting to the unique characteristics of individual datasets, leading to improved generalization across diverse clients. This feature is particularly critical in biological data, where variability between datasets commonly arises from differences in laboratory conditions, equipment, and methodologies.

4.2. Bacterial classification accuracy

The performance comparison between the proposed CNN-FL framework and traditional CNN models is illustrated in Fig. 3. As observed, Fig. 3 highlights several key performance metrics through scatter plots and radar charts. This figure illustrates various aspects of the framework's performance, focusing on key metrics such as F_1-score, recall, and precision. The evaluation is conducted under different configurations to highlight the advantages of the CNN-FL framework, particularly in decentralized environments. This method assumes that all data in the network can be collected and trained by a single centralized node, which is an important consideration. Fig. 3A compares true labels (blue) and predicted labels (brown) for bacterial counts using a centralized CNN across three laboratories. Misclassifications are notable for *Clostridium perfringens* (6), *Enterococcus faecium* (8), *Escherichia coli* (9), and *Lactobacillus crispatus* (12), indicating prediction errors. The shape of bacteria, such as rod-shaped *Clostridium* and spherical *Cocci*, affects CNN performance. Notably, this centralized approach shows slightly poorer performance than that of the proposed CNN-FL framework with 2 and 3 clients. Fig. 3B shows our proposed CNN-FL framework with 2 clients.

The accuracy of the results was rigorously validated, and the dataset utilized in this study was meticulously curated to ensure its high quality. The bacterial classification accuracy, as depicted in Fig. 3, illustrates the framework's capability to manage diverse and complex bacterial morphologies effectively. The observed misclassifications, such as those involving *Lactobacillus johnsonii* and *Clostridium perfringens*, underscore the challenges associated with distinguishing bacteria that exhibit similar morphological characteristics. These outcomes were anticipated given the inherent limitations of image-based

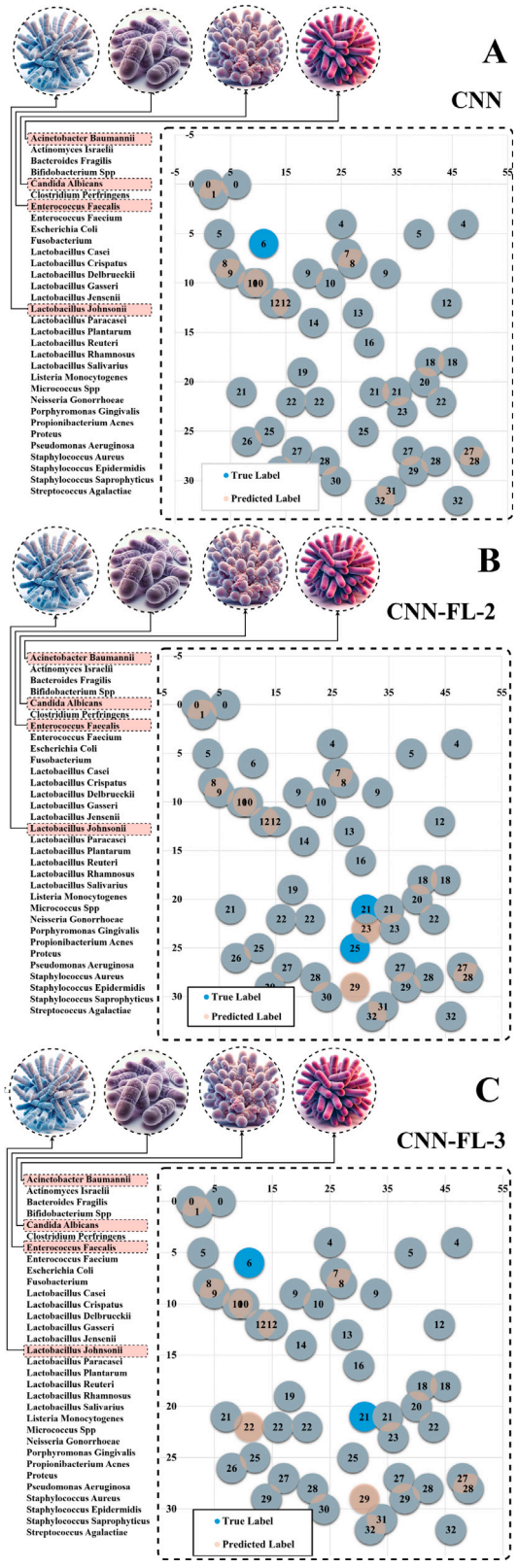

Fig. 3. A: Centralized CNN model predicted versus actual bacterial counts; B: CNN-FL framework with 2 clients predicted versus actual counts; C: CNN-FL framework with 3 clients predicted versus actual counts.

classification, in which shape and color similarities can present difficulties even for advanced models. Nevertheless, the overall enhancement in accuracy achieved with the CNN-FL framework, particularly in the 3-client configuration, underscores the robustness of the proposed approach. The incorporation of additional clients introduces a more diverse training dataset, which subsequently improves the model's capacity to differentiate between bacterial species.

Misclassifications are fewer and less pronounced, highlighting the framework's effectiveness in improving accuracy. Notable errors include *Lactobacillus johnsonii* (21) and *Propionibacterium acnes* (25). Fig. 3C displays results from the CNN-FL framework with 3 clients, showing further reduction in misclassifications compared to the centralized and 2-client models. Notable errors include *Clostridium perfringens* (6) and *Lactobacillus johnsonii* (21). This enhancement underscores the CNN-FL framework's robustness in addressing prediction errors related to bacterial shapes and overall improved classification performance. The proposed CNN-FL framework with 2 and 3 clients slightly reduces bacterial misclassification errors compared to the centralized CNN, highlighting the impactful role of client collaboration in improving accuracy and robustness in handling diverse bacterial shapes.

Fig. 4 presents radar charts comparing the performance metrics, including precision, recall, and F1-score of the centralized CNN model and the proposed CNN-FL frameworks with 2 and 3 clients. Fig. 4A illustrates the centralized CNN model. The chart shows relatively high precision but lower recall, leading to lower F1-scores. This indicates that while the model is good at identifying positive instances, it struggles to capture all true positives, especially for bacteria with complex shapes like rod-shaped *Clostridium* and spherical *Cocci*. Fig. 4B depicts the performance of the CNN-FL framework with 2 clients. The radar chart demonstrates improved balance between precision and recall, resulting in higher F1-scores. This suggests that the distributed approach enhances the model's ability to consistently classify and predict bacterial counts more accurately, mitigating some of the shortcomings observed in the centralized CNN model. Fig. 4C shows the CNN-FL framework with 3 clients. This configuration demonstrates superior performance, achieving consistently high precision, recall, and F1-scores across all bacterial classifications. The inclusion of additional clients further enhances the model's robustness and accuracy in managing diverse bacterial morphologies, thereby highlighting the efficacy of collaborative learning in improving both predictive performance and reliability. The radar charts highlight the superiority of the CNN-FL frameworks over the centralized CNN model, particularly with the addition of more clients, which significantly boosts the model's precision, recall, and F1-scores.

Table 2 presents a comparative analysis of the classification performance for three methods: CNN-FL with one client, CNN-FL with two clients, and a centralized CNN approach. The table summarizes key metrics such as mean precision, recall, and F1-score, along with their minimum, maximum, and standard deviation values. The CNN-FL methods, particularly with two clients, generally exhibit slightly better performance metrics and lower variability compared to the centralized CNN, which still maintains high accuracy but with marginally higher error rates in certain cases. The table highlights the robustness of FL methods, especially in scenarios with diverse and complex bacterial datasets.

4.3. Data exchange and error rates

The integration of IoBNT and FL within the proposed framework establishes a synergistic mechanism that promotes collaborative learning across diverse data sources. This enhances the precision and granularity of models for conducting detailed analyses of environmental data and micro-level biological components. The adoption of FL substantially optimizes data transmission by facilitating decentralized learning, which significantly reduces bandwidth consumption. Moreover, the implementation of IoBNT notably minimizes error rates in the extraction of biological data, ensuring precise and accurate data collection. This level of precision is crucial for developing highly representative DTs, enabling more reliable simulations and analyses. Additionally, FL allows

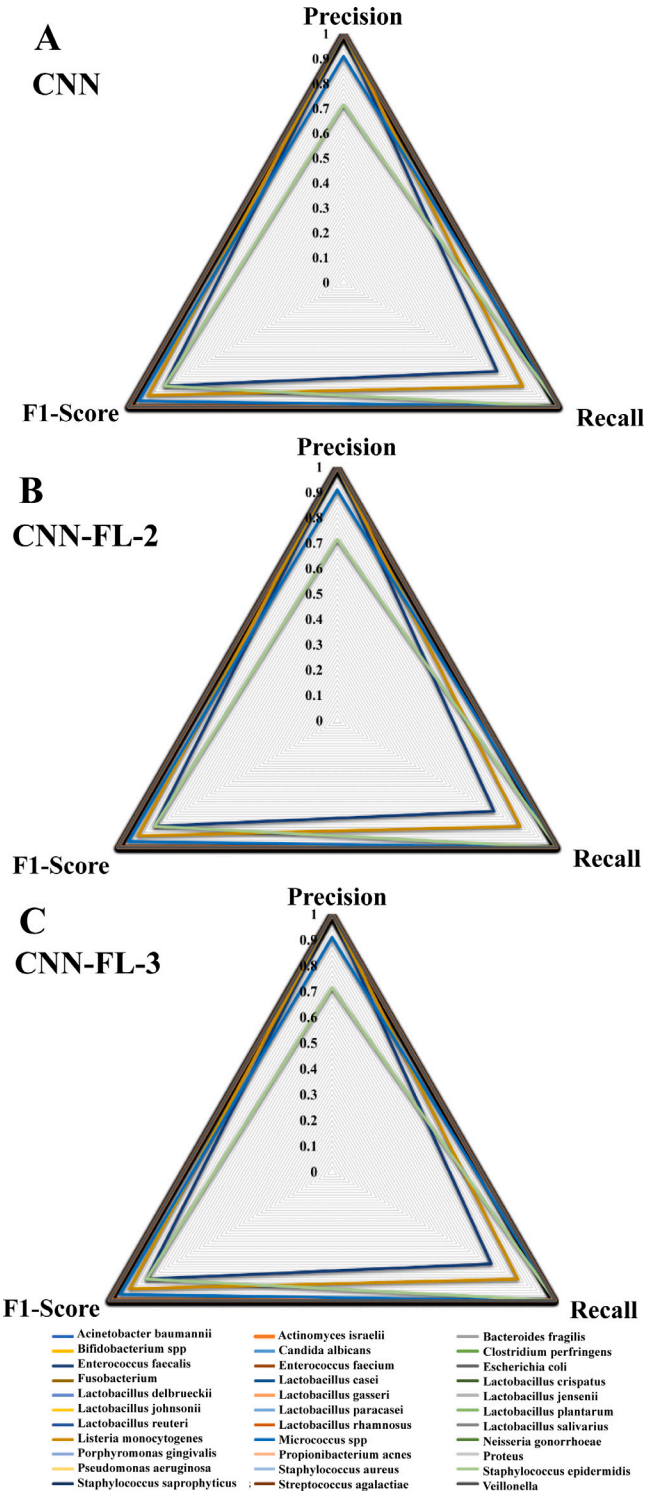

Fig. 4. Performance Comparison Using Radar Charts; A: Precision, recall, and F1-score for the centralized CNN model; B: Precision, recall, and F1-score for the CNN-FL framework with 2 clients; C: Precision, recall, and F1-score for the CNN-FL framework with 3 clients.

various clients, such as laboratories and hospitals, to collaboratively engage in microorganism pattern recognition across multiple locations, thereby improving operational efficiency and further reducing error rates [32]. Sensors embedded within the IoBNT network play a pivotal role in gathering detailed biological data and transmitting it to the local servers of each client. This initial data acquisition by IoBNT nodes establishes a strong foundation for comprehensive analysis and informed decision-making. These enhancements, which include bandwidth optimization via FL and error rate reduction in biological data extraction through IoBNT, are elaborated in the subsequent sections.

Table 2
Comparative analysis of classification methods.

Metric	CNN-FL (2 client)	CNN-FL (3 clients)	Centralized CNN
Precision (mean)	0.987	0.988	0.986
Precision (min)	0.800	0.714	0.833
Precision (max)	1.000	1.000	1.000
Recall (mean)	0.985	0.986	0.988
Recall (min)	0.800	0.714	0.857
Recall (max)	1.000	1.000	1.000
F1-Score (mean)	0.986	0.986	0.986
F1-Score (min)	0.800	0.833	0.909
F1-Score (max)	1.000	1.000	1.000
Standard Deviation (Precision)	0.041	0.049	0.044
Standard Deviation (Recall)	0.047	0.054	0.035
Standard Deviation (F1-Score)	0.039	0.041	0.029
Weighted Avg. Precision	0.987	0.989	0.987
Weighted Avg. Recall	0.985	0.986	0.986
Weighted Avg. F1-Score	0.986	0.986	0.986

4.3.1. Significant bandwidth optimization

Our framework achieves remarkable bandwidth reduction by distributing the computational load across clients. This approach effectively reduces the bandwidth required for data transfer, optimizing resource usage. Key challenges in biotechnology and healthcare, such as scalability, accuracy, bandwidth, and privacy, are addressed through the integration of IoBNT, CNN, and FL technologies. By leveraging FL, our framework eliminates the need to transfer large image datasets to a central server for training, leading to substantial bandwidth savings. Instead, only the model weights and parameters are transmitted, significantly reducing data transfer volume and enhancing overall efficiency and scalability. The framework efficiently manages a dataset of 3.5 GB comprising 2,033 images by leveraging FL, significantly reducing data transfer requirements compared to centralized training methods. In a centralized training scenario, transferring the entire dataset between laboratories and servers necessitates each client to send approximately 1.75 GB of data, even with just two clients involved, resulting in substantial data transfer volumes. However, by employing FL, only the model weights and parameters are transmitted, drastically reducing uplink and downlink data transfer requirements and enhancing overall efficiency.

The MobileNetV2 model [72], used in our framework, has about 2.2 million parameters, which roughly translates to 8.8 MB per model (assuming 32-bit precision). Therefore, in each round, the total data transmitted per client is just 8.8 MB, a substantial reduction from the gigabytes required for image transfer. Thus, this mechanism leads to a significant reduction in the load on the communication channel, allowing the use of simpler and more cost-effective communication infrastructures. From an economic perspective, the reduced data transfer enhances the usability of the proposed framework. Furthermore, the efficiency in data handling supports rapid scaling, enabling the addition of numerous clients without compromising performance or incurring significant additional costs. Additionally, transmitting heavy data in real-time often poses implementation and hardware capacity problems. However, by reducing the data size, our framework maintains very fast training speeds while preserving privacy, overcoming these challenges effectively. Consequently, this translates to bandwidth savings per client of approximately 1.74 GB, reducing network traffic by more than 99% (Table 3).

Extending this to a larger scenario involving 20 million RGB images and 50 clients, the bandwidth savings are even more pronounced.

Table 3
Detailed bandwidth savings information.

Description	Details
Small Scale (2 Clients)	
Dataset size	2,033 images, 3.5 GB
Max. transmitted data per client	Centralized: 1.75 GB
Max. transmitted data per client per learning round	FL: 8.8 MB
Bandwidth savings per transmission	1.7324 GB (99%)
Large Scale (50 Clients)	
Dataset size	2 m images, 3.44 TB
Max. transmitted data per client	Centralized: 68.8 GB
Max. transmitted data per client per learning round	FL: 8.8 MB
Bandwidth savings per transmission	137.5824 GB (99.98%)

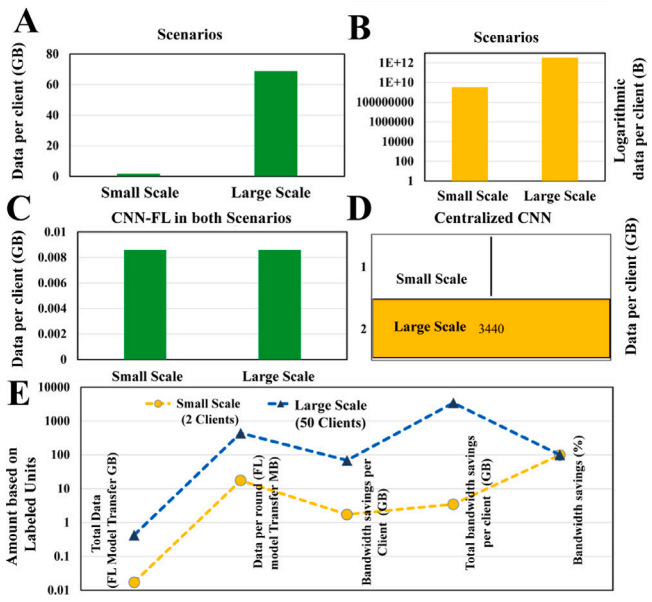

Fig. 5. Optimization of bandwidth savings and noise reduction in data transfer using CNN-FL with IoBNT technologies; A: Data size of image transfer for small-scale and large-scale datasets; B: Total dataset size for both scenarios from a logarithmic perspective; C: Bandwidth usage in both scenarios for the proposed CNN-FL framework; D: Bandwidth usage in both scenarios for the Centralized CNN; E: Bandwidth optimization achieved for both small and large-scale scenarios.

Assuming each image would take at least 1MB minimum (assuming they are of high resolution), the total size of the dataset is 20 TB.

If centralized training were employed, each of the 50 clients would need to send around 400 GB of image data to the central server, calculated as:

$$\frac{20\,\text{TB}}{50\,\text{clients}} = 400\,\text{GB/client}. \tag{15}$$

In contrast, with our CNN-FL framework, each client only needs to send the updated model weights. Given the MobileNetV2 model's size of approximately 8.8 MB per round for uplink, and the same amount for downlink, the total data per client per round is 17.6 MB, calculated as:

$$8.8\,\text{MB (uplink)} + 8.8\,\text{MB (downlink)} = 17.6\,\text{MB/client}. \tag{16}$$

This represents a significant bandwidth saving, reducing the data transmitted from 400 GB to just 17.6 MB. Consequently, the bandwidth saving is approximately 399.9824 GB, calculated as:

$$400\,\text{GB} - 17.6\,\text{MB} \approx 400\,\text{GB} - 0.0176\,\text{GB} = 399.9824\,\text{GB}. \tag{17}$$

This translates to a reduction of over 99.9956% in data transfer requirements, calculated as:

$$\left(1 - \frac{17.6\,\text{MB}}{400\,\text{GB}}\right) \times 100\% \approx \left(1 - \frac{0.0176\,\text{GB}}{400\,\text{GB}}\right) \times 100\% \approx 99.9956\%. \tag{18}$$

Fig. 5A illustrates the volume of image transfer for two distinct scenarios: a small-scale dataset and a large-scale dataset comprising 20 million images distributed among 50 clients. In small-scale scenarios, we achieved substantial bandwidth savings, thereby demonstrating the practical efficacy of our framework. These preliminary findings provide a foundation for evaluating the framework's performance in large-scale scenarios. By leveraging the practical results obtained from smaller setups, we emphasize the scalability and efficiency of the proposed approach. Fig. 5B presents the total dataset size for both small-scale and large-scale scenarios using a logarithmic scale, which highlights the significant disparities in data volume between the two scenarios. Fig. 5C depicts the bandwidth usage in both scenarios for the proposed framework. Additionally, Fig. 5D shows the total dataset size per client for both small-scale and large-scale setups in a centralized CNN. Fig. 5E demonstrates the bandwidth optimization achieved in both scenarios using our CNN-FL framework. In the small-scale scenario, the bandwidth requirement per client is drastically reduced from 1.75 GB to just 8.8 MB, representing savings exceeding 99%. Similarly, in the large-scale scenario involving a dataset of 20 million images distributed among 50 clients, the bandwidth requirement per client is reduced from 400 GB to 17.6 MB, achieving an extraordinary savings of 99.9956%. Consequently, our FL approach, enhanced by IoBNT, not only ensures scalable and cost-effective training but also provides a robust and efficient solution for managing extensive image datasets across distributed networks.

By utilizing IoBNT, which enhances the fidelity and efficiency of data communication, the framework achieves a seamless and noise-reduced data transfer process. This integration ensures reliable connectivity and a consistent flow of data, effectively mitigating network congestion while maintaining data privacy. Consequently, the FL approach, strengthened by IoBNT, delivers a scalable and cost-effective training solution that is also dependable and efficient for managing large-scale image datasets across distributed networks.

4.3.2. Optimizing error rates in biological data transfer

Our framework employs IoBNT technology for nanoscale and molecular communication to optimize error rates in biological data transfer. Traditional IoT systems exhibit error rates ranging from 1% to 5% [26]. These error rates can result in significant data losses, ranging from 35 MB to 175 MB when transferring a 3.5 GB dataset, thereby compromising data fidelity. Fig. 6F compares error rates and data loss between IoT and our proposed framework. The gray section on the left represents IoT protocols (IEEE 802.11), with high error rates (1%–5%) and significant data loss (up to 175 MB). The white section on the right depicts our proposed IoBNT-based framework (IEEE P1906.1), showcasing minimal error rates (0.01%–0.1%) and data loss (up to 3.5 MB).

For our proposed dataset size of 3.5 GB (or 3,500 MB), the data loss due to these error rates can be calculated as follows:

- For an error rate of 1%, the data loss is 35 MB.
- For an error rate of 5%, the data loss is 175 MB.

Thus, conventional IoT systems experience data losses ranging from 35 MB to 175 MB when transferring the entire 3.5 GB dataset.

In contrast, IoBNT technology, guided by IEEE P1906.1 standards for nanoscale and molecular communication frameworks, demonstrates significantly lower error rates between 0.01% and 0.1%. For the same dataset size, the data loss due to these error rates can be calculated as follows:

- For an error rate of 0.01%, the data loss is 0.35 MB.
- For an error rate of 0.1%, the data loss is 3.5 MB.

Thus, IoBNT systems experience minimal data losses ranging from 0.35 MB to 3.5 MB for the same dataset size, ensuring high data fidelity.

These results confirm the efficacy of our IoBNT framework in optimizing error rates, ensuring data integrity, and enhancing the overall efficiency of biological data transfer, making it a highly effective solution for modern biotechnological applications.

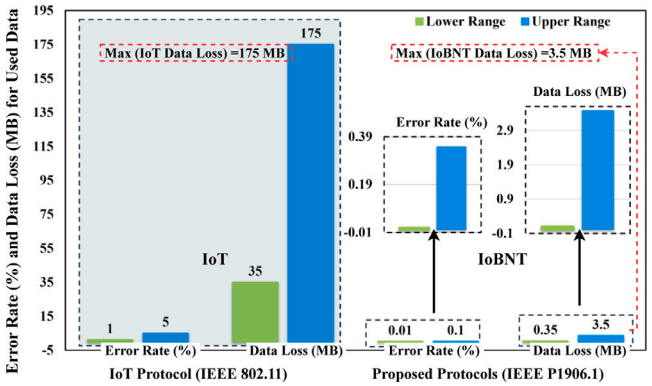

Fig. 6. Comparison of error rates and data loss between IoT and IoBNT technologies in biological data transfer.

4.4. The powerful synergy between local CNN models and FL

We introduce CNN-FL to leverage the strengths of both CNN and FL for advanced biological data processing and bacteria analysis [31]. This synergistic combination of local CNN models and FL revolutionizes the processing of biological data, particularly in handling bacteria. By integrating FL with CNNs, the system is significantly enhanced in IoT environments, enabling it to handle extensive data from diverse sources without the need for centralizing data storage. This approach ensures data privacy, as sensitive biological information remains localized. Specifically, local CNN models, such as MobileNetV2 [72], process data with high efficiency, thereby enhancing the global model's accuracy by integrating insights from diverse datasets. Furthermore, this system effectively addresses critical challenges in biotechnology, including scalability, accuracy, bandwidth optimization, and privacy. By distributing the data load across multiple clients, the CNN-FL framework achieves superior load management and more efficient data processing. For instance, in a 2-client configuration, each client manages approximately 1017 images, while in a 3-client configuration, each client handles around 678 images. This approach not only improves system efficiency but also mitigates privacy concerns by keeping data local to each client, thereby minimizing the need for extensive data transfers and ensuring robust data security.

This architecture includes 53 convolutional layers organized into 17 inverted residual blocks, significantly reducing computational load. Each block starts with a lightweight depthwise convolution followed by a pointwise convolution that expands and then compresses the channels. The model is topped with a global average pooling layer and a dense layer with 33 units corresponding to the number of bacterial classes, providing robust classification outputs with minimal computational overhead. Furthermore, this combination leads to a more efficient and advanced approach to creating DTs, where virtual models of 33 types of bacteria can be created and analyzed in real-time. Consequently, this paves the way for more energy-efficient and sophisticated methods to realize DTs, enhancing our ability to monitor, understand, and manipulate biological systems with unprecedented precision and efficiency. The integration allows for the precise extraction and dynamic response to data changes at molecular and cellular levels, thereby dramatically improving the performance of DTs to a precision of 98.7% with 2 clients and 98.8% with 3 clients. The continuous monitoring and immediate adjustments enabled by IoBNT ensure more accurate and responsive simulations, which are essential for advancing biotechnological research and applications.

Fig. 7 presents three confusion matrices corresponding to the centralized CNN model, the proposed CNN-FL framework with 2 clients, and the CNN-FL framework with 3 clients, respectively. These confusion matrices provide a comparative perspective on the classification performance of different model architectures, offering valuable insights into the advantages of FL frameworks. Fig. 7A illustrates the confusion matrix for the centralized CNN model, where the diagonal elements, representing correct classifications, demonstrate high accuracy for several bacterial species. This result suggests that the centralized CNN model is generally effective in accurately identifying many bacteria, serving as a robust baseline. However, the off-diagonal elements reveal instances of misclassification, underscoring the challenges associated with distinguishing bacterial species that share similar features or morphological traits. For example, *Staphylococcus Aureus* is misclassified as *Clostridium Perfringens*, likely due to similarities in specific morphological or staining characteristics that confuse the model. Similarly, *Proteus* is misidentified as *Propionibacterium Acnes*, and *Pseudomonas Aeruginosa* is mistaken for *Staphylococcus Aureus*. These misclassifications highlight the limitations of the centralized CNN model in addressing complex bacterial differentiation tasks, which may arise from overlapping features or insufficient discriminative capability within the feature extraction layers. Addressing these errors may require the adoption of more advanced feature extraction techniques or the integration of enhanced training datasets to improve classification accuracy in challenging cases.

Furthermore, Fig. 7B depicts the confusion matrix for the CNN-FL framework with 2 clients, where the misclassifications are similar to those observed in the centralized CNN model. The similarity in these misclassifications implies that while FL provides significant advantages in terms of privacy and data decentralization, it does not inherently address the classification challenges posed by certain bacterial species. For instance, *Micrococcus Spp* is misclassified as *Lactobacillus Salivarius*, which may result from insufficient diversity in the local datasets of individual clients, thereby limiting the model's capacity to learn distinctive features for each bacterium. Other notable misclassifications include *Staphylococcus Aureus* as *Porphyromonas Gingivalis* and *Clostridium Perfringens* as *Staphylococcus Aureus*. These errors underscore the necessity for improved data-sharing mechanisms or augmentation strategies within the FL framework to enhance classification accuracy. Fig. 7C illustrates the confusion matrix for the CNN-FL framework with 3 clients, showing a notable reduction in misclassifications compared to both the centralized CNN model and the CNN-FL framework with 2 clients. The decrease in misclassifications indicates that increasing the number of clients in the FL setup contributes to a more robust and generalized model, likely due to the integration of more diverse data. However, certain errors persist, such as *Listeria Monocytogenes* being misclassified as *Clostridium Perfringens*, *Staphylococcus Aureus* as *Clostridium Perfringens*, and *Staphylococcus Aureus* also being misclassified as *Lactobacillus Salivarius*. These remaining misclassifications highlight that although FL improves overall accuracy, specific bacterial species continue to pose significant classification challenges, possibly due to intrinsic morphological similarities or limitations in the training data.

One of the more unexpected findings in this study was the substantial improvement in convergence speed observed in the CNN-FL models. Although faster convergence was anticipated due to the decentralized nature of FL, the reduction in training rounds from 120 in the centralized CNN to just 40 in the CNN-FL framework is particularly noteworthy. This outcome suggests that the aggregation of knowledge across clients not only enhances accuracy but also significantly accelerates the learning process, warranting further investigation. Another unexpected result was the model's performance in classifying specific bacterial species, such as *Staphylococcus Aureus*, which was frequently misclassified across all models (Fig. 7). This finding highlights the need for further refinement of the feature extraction layers, especially for bacteria with similar morphological characteristics. Addressing these challenges will be critical to improving the model's overall robustness in practical applications. This study contributes to the existing body of literature by demonstrating the feasibility and effectiveness of applying CNN-FL to bacterial classification, a domain that has traditionally relied

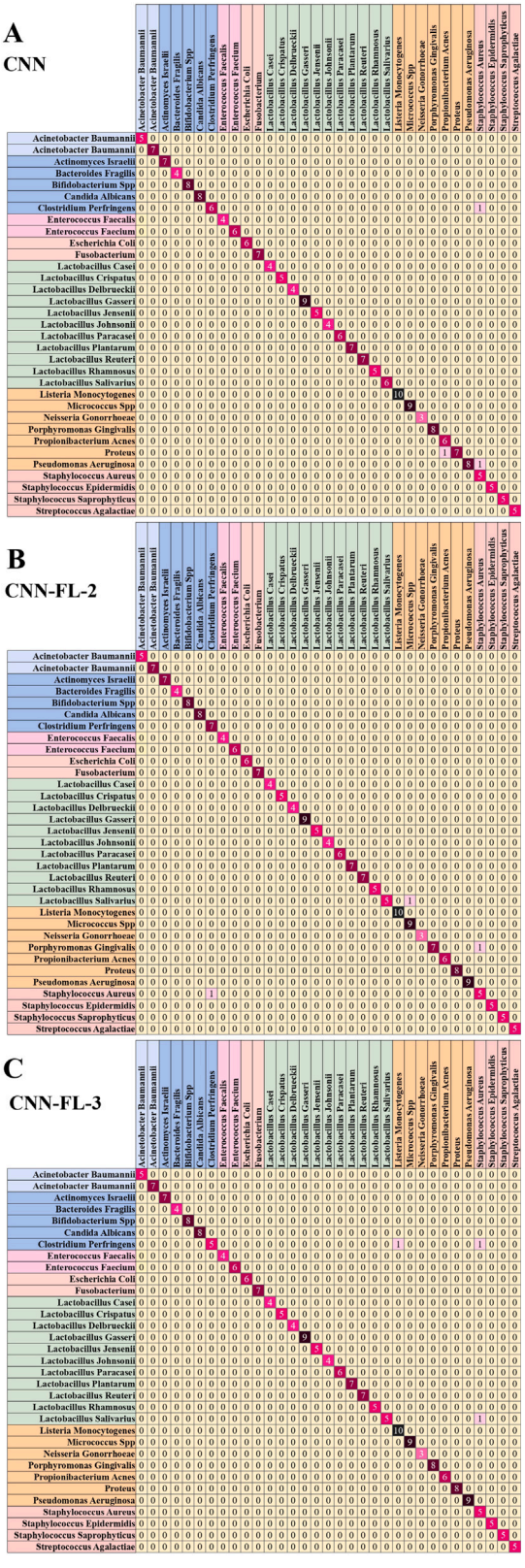

Fig. 7. Confusion matrices illustrating the classification performance of different models; A: The conventional centralized CNN model; B: The global model in the CNN-FL framework with 2 clients; C: The global model in the CNN-FL framework with 3 clients.

on centralized data processing models. The integration of IoBNT with FL within this framework represents an innovative contribution, enabling more efficient data processing and bandwidth optimization. By decentralizing the learning process, this framework not only preserves data privacy but also enhances model performance.

Based on the provided confusion matrices, several bacteria have not been classified or mistaken for others. The frequent misclassifications highlight areas where the model's feature extraction and classification processes could be further refined. These include *Streptococcus Agalactiae*, *Staphylococcus Saprophyticus*, *Staphylococcus Epidermidis*, *Neisseria Gonorrhoeae*, *Lactobacillus Rhamnosus*, *Lactobacillus Reuteri*, *Lactobacillus Plantarum*, *Lactobacillus Paracasei*, *Lactobacillus Johnsonii*, *Lactobacillus Jensenii*, *Lactobacillus Gasseri*, *Lactobacillus Delbrueckii*, *Lactobacillus Crispatus*, *Lactobacillus Casei*, *Fusobacterium*, *Escherichia Coli*, *Enterococcus Faecium*, *Enterococcus Faecalis*, *Candida Albicans*, *Bifidobacterium Spp*, *Bacteroides Fragilis*, *Actinomyces Israeli*, and *Acinetobacter Baumannii*. This comprehensive list underscores the complexity and diversity of bacterial species, which require sophisticated models to achieve high classification accuracy. The most frequently misclassified bacteria is *Staphylococcus Aureus*. Its frequent misclassification highlights a critical area for improvement, as accurate identification of this bacterium is crucial for clinical diagnostics and treatment. It is mistaken for *Clostridium Perfringens* in the centralized CNN model, misclassified as *Porphyromonas Gingivalis* in the CNN-FL framework with 2 clients, and misclassified as both *Clostridium Perfringens* and *Lactobacillus Salivarius* in the CNN-FL framework with 3 clients. The consistent misclassification of *Staphylococcus Aureus* across different models highlights the need for targeted improvements in the feature extraction and classification algorithms to enhance its identification. This indicates that *Staphylococcus Aureus* poses the greatest challenge for accurate classification across all models. Addressing this challenge is essential for improving the overall performance of bacterial classification models, which could involve incorporating more specific biomarkers or advanced learning techniques.

4.5. Monitoring and predicting DTs

DTs in bioprocess monitoring and prediction exhibit considerable effectiveness by leveraging real-time data and advanced modeling techniques. These capabilities provide profound insights into the properties of bioproducts and the dynamics of bioprocesses, ensuring process continuity and maintaining product integrity, which are essential in biotechnological applications [64]. DTs are particularly adept at real-time monitoring, anomaly detection, and predictive maintenance. Nevertheless, the deployment of DTs is accompanied by significant challenges. Developing accurate models for dynamic biological systems amidst large, complex datasets presents a notable difficulty. The intricate nature of biological data, combined with the demand for substantial computational resources, necessitates the use of sophisticated algorithms and robust computational infrastructure. Despite these obstacles, the potential advantages of DTs in delivering precise and real-time insights into bioprocesses emphasize their critical role in advancing biotechnological research and applications.

Fig. 8 illustrates the user dashboard designed for accessing DTs of recognized bacteria. The system begins with the Database (Data Storage), where graphic elements and relevant data for generating DTs are stored. This database acts as a central repository, storing digital models and metadata related to different bacterial species. The External Data Sources block is responsible for integrating real-time location recognition and predictive data from various sources, ensuring that the DTs are updated with the latest environmental and contextual information. These data sources are crucial for maintaining the accuracy and relevance of the DTs. The API Gateway (Data Exchange) facilitates communication between the database and other system components. It manages data requests and responses, ensuring efficient data flow and exchange. The Web Server (Data Processing) handles the processing of

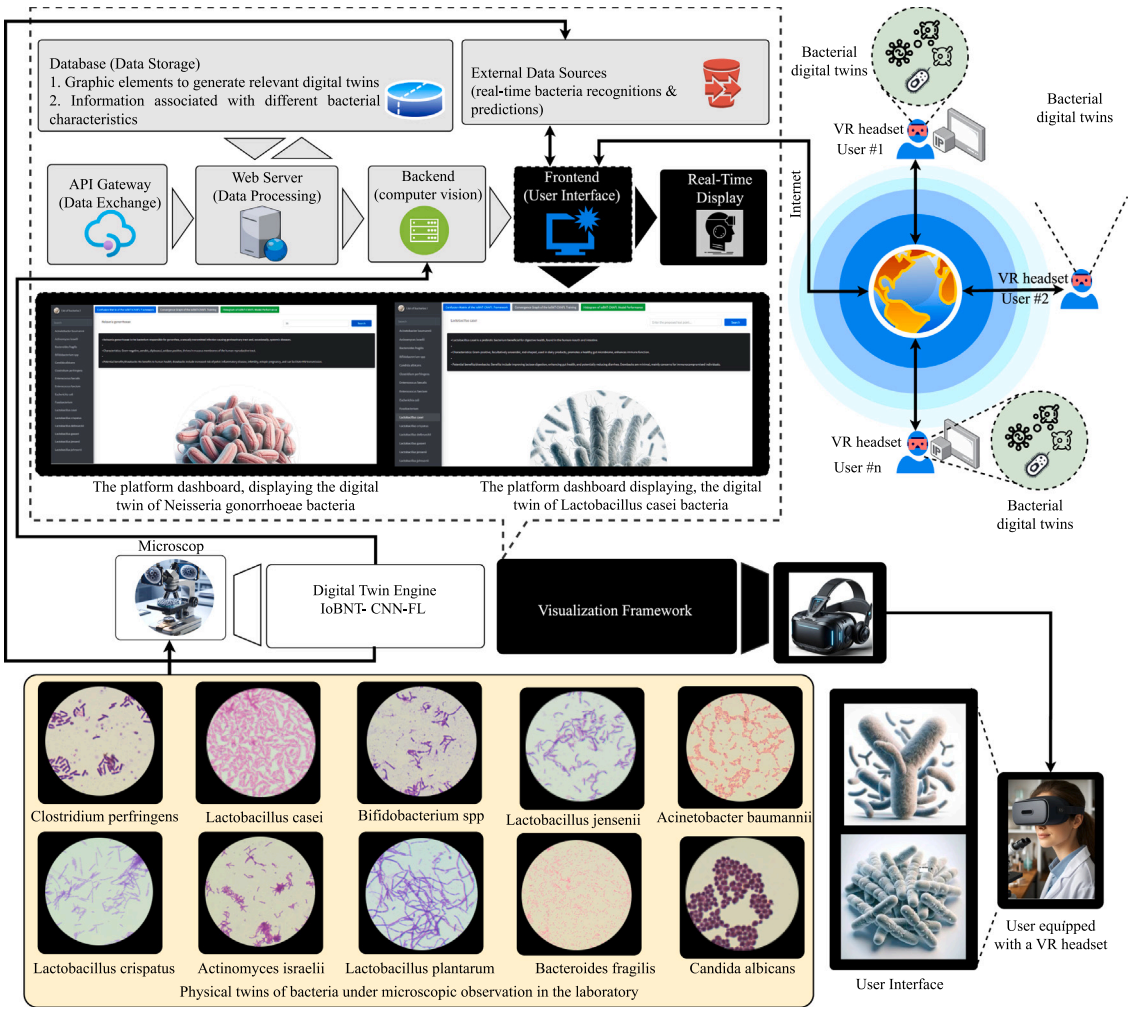

Fig. 8. User Dashboard for Accessing DTs of Recognized Bacteria. The dashboard backend provides users with an output interface for the framework, presenting DTs of recognized bacteria. End users can access the results via a VR headset or monitor through an HTML page. This desktop interface offers a user-friendly experience, enabling real-time access and observation of results.

incoming data, converting raw inputs into structured formats that can be used for visualization. It processes data from both the database and external sources, preparing it for backend analysis. User Interface is the layer where users interact with the system. It provides an HTML-based interface that supports multiple devices.

This dashboard acts as the primary interface for users to interact with the framework's output. Users can access the results through a Virtual Reality (VR) headset for an immersive experience or via a standard monitor through an HTML-based interface, ensuring flexibility and ease of use. The desktop interface is specifically designed to offer a seamless and intuitive user experience, allowing real-time access and observation of results. This setup caters to a wide range of users, including researchers and medical professionals, by providing immediate and straightforward access to detailed bacterial data. The dual access methods (VR and HTML) ensure that the users can choose their preferred way of interacting with the data, making the dashboard a versatile tool for various applications.

5. Discussion

In this work, we present a highly efficient DT framework powered by CNN-FL and IoBNT to realize bacterial DTs. These DT models must accurately reflect their dynamics and interactions, representing biological systems in a scalable and secure manner. Predicting, optimizing, and analyzing the performance of IoBNT and biological systems through methods and simulation tools constitute a crucial research area. Potential research directions include developing scalable simulation platforms and ML techniques to improve predictions, incorporating advanced data analytics, and enhancing model accuracy for complex, multi-scale biological systems [28]. Our proposed framework offers a robust solution for optimizing bandwidth, reducing error, processing biotechnological data, and digitizing biological assets. By leveraging CNN, FL, and IoBNT technologies, this approach addresses the challenges of employing DTs at nano and micro scales for modeling biosystems and biological assets such as bacteria. Integrating IoBNT with deep learning algorithms like FL and CNN significantly enhances the dependability, reliability, and efficiency of DTs in the biotechnology industry.

5.1. Addressing identified gaps: Framework performance and key features

Our proposed framework focuses on overcoming key challenges in the biotechnology domain, particularly when dealing with complex and diverse datasets, such as bacterial images collected from multiple sources. The framework offers a robust and scalable solution that effectively addresses challenges related to computational complexity, data privacy, and concerns associated with real-world deployment. Scalability is an essential consideration in modern frameworks designed for large-scale data processing, particularly in biotechnology, where data is frequently collected from diverse sources. The FL architecture is

deliberately selected to ensure scalability in contexts where datasets are extensive and distributed across multiple laboratories or IoBNT devices.

Moreover, the distributed architecture of FL facilitates local data processing on each IoBNT device and enables real-time updates of DTs without necessitating data centralization. This localized processing ensures that as the number of data points or IoBNT devices grows, the computational load is distributed across multiple clients rather than concentrated on a single centralized server. This approach effectively alleviates potential bottlenecks when scaling to larger datasets or incorporating additional clients. Each device contributes to the training process by transmitting model updates instead of raw data, thereby significantly reducing network traffic and enhancing the system's scalability. Furthermore, the capacity to update DTs in real time is particularly critical for biotechnology applications, where rapid analysis and decision-making are imperative. The scalability of this framework makes it well-suited for scenarios involving extensive networks of IoBNT devices and laboratories, where each client supports the global model without overwhelming the system.

While the integration of CNNs with FL and IoBNT brings significant benefits in terms of image analysis and data integration, it also introduces a degree of computational complexity. CNNs, especially when applied to high-resolution bacterial images, are computationally intensive. However, this framework addresses this complexity through a carefully designed preprocessing algorithm that ensures consistent and standardized image inputs. Biological data, such as bacterial images collected from various sources (e.g., microscopes), often suffers from inconsistent image quality, with variations in resolution, contrast, and color balance. These inconsistencies can negatively impact the performance of CNNs if not properly managed. To mitigate this, advanced image preprocessing techniques are used to standardize the image data. This ensures that regardless of the data source, the images maintain uniformity, which is critical for accurate and reliable analysis. By normalizing and standardizing the images, the CNN can focus on the biologically relevant features, such as bacterial morphology and texture, rather than being affected by noise or image quality issues.

Furthermore, the choice of CNN architecture plays a key role in managing computational complexity. Lightweight CNN models, such as MobileNetV2, are specifically designed to reduce computational load without sacrificing accuracy. These models use fewer parameters and require less memory, making them well-suited for deployment on IoBNT devices that may have limited computational resources. By leveraging MobileNetV2, the framework achieves an optimal balance between performance and efficiency, ensuring its practicality for deployment in real-world biotechnology environments without overburdening local devices. The federated architecture of the framework further aids in managing computational complexity. As each IoBNT device processes only its local data and contributes to the global model by transmitting model weights instead of raw data, the overall computational load is effectively distributed across the network. This distributed processing ensures that the complexity of integrating CNNs with FL does not overwhelm any single system. Instead, the workload is spread across multiple devices, each handling a portion of the computational requirements, thus improving overall efficiency.

The deployment of AI frameworks in real-world biotechnology settings presents numerous challenges, particularly concerning data privacy, data quality, and computational resources. This framework is designed to address these challenges head-on, ensuring that it is practical and effective for use in diverse environments. One of the primary concerns in biotechnology applications is the variability of data quality. Bacterial images are often collected under varying conditions, leading to differences in image quality, resolution, and color. In terms of data privacy, the use of FL ensures that sensitive biological data remains localized. Data privacy is a critical concern in real-world deployments, especially in fields such as biotechnology where data may be subject to strict regulatory requirements. By keeping the data on local devices and only sharing model updates (rather than the raw data itself), this framework ensures that data privacy is maintained throughout the training process. This approach also minimizes the risk of data breaches, as no centralized database of sensitive information exists. Instead, the data remains under the control of each participating laboratory or IoBNT device.

The framework is also designed to overcome computational resource constraints found in real-world applications. Many IoBNT devices, especially those in remote or limited-resource settings, have restricted processing power and memory. To enable deployment on such devices, lightweight CNN architectures and distributed learning strategies are used to reduce computational load on each device. By distributing processing tasks across multiple clients and leveraging efficient models, the framework remains effective even in resource-limited settings. Furthermore, the framework is highly scalable, capable of accommodating an increasing number of clients as data volumes grow, with no predefined upper limit. The current setup with three clients is not a limitation, as the architecture allows adding more clients through FL, effectively distributing the computational load across the network. By utilizing lightweight CNNs like MobileNetV2, the framework reduces the processing burden on IoBNT devices. Only model updates, not raw data, are shared, minimizing bandwidth use. With 90% accuracy, the framework is robust and ready for real-world biotechnology applications, offering practical and scalable solutions across varied environments.

Embedding MobileNetV2 as our CNN model, combined with FL, yields promising results in creating bacterial DTs. Pre-trained on ImageNet and fine-tuned on bacterial images, this CNN processes data in batches of 32, with each image resized to 224×224 pixels. Its compact architecture, with approximately 2.2 million parameters, enables efficient training and inference across distributed nodes in an FL setup. This approach achieves over 98.7% accuracy for 33 bacterial classes, as evidenced by metrics such as accuracy, precision, and recall during training. Integrating MobileNetV2 allows for faster convergence and reduced communication overhead during federated updates, supporting efficient and scalable processing capabilities for real-time creation of bacterial DTs across multiple clients on mobile platforms. Its compact and efficient design positions our framework well for future commercial applications, driving widespread adoption in healthcare and environmental monitoring.

Moreover, using FL with CNN in the proposed framework significantly improves training speed and accuracy compared to traditional centralized CNN models. As a result, the CNN-FL framework with 2 and 3 clients achieves 95% accuracy within the first 20 rounds, whereas the centralized CNN model requires over 110 epochs to reach the same level. Additionally, our framework attains over 98% accuracy in only 40 rounds, while centralized CNNs need 120 epochs for similar results. This dramatic reduction in training rounds underscores our optimization strategies' effectiveness, enabling faster deployment and iteration of models across multiple laboratories. Therefore, achieving high accuracy in significantly fewer rounds allows for more efficient use of computational resources and reduces the time required for model training, particularly beneficial in environments where rapid deployment and iteration are critical. The superior performance of the CNN-FL framework highlights its potential for real-world applications, where optimizing convergence speed and accuracy is essential.

The foundation of our framework is rooted in computer vision and pattern recognition, enabling it to function effectively as long as an adequate number of species images are available for training. The framework's ability to handle different data types makes it highly adaptable to various biological assets, as it does not rely on the specific type or properties of microorganisms. Its strength lies in detecting patterns in the input data, regardless of species characteristics. Expanding this framework to encompass other biological assets, such as tissues, organs, or entire biological systems, is feasible by applying the same principles of image-based pattern recognition and deep learning. The

adaptability of the framework is attributed to the versatility of CNNs, which are capable of handling the increased complexity associated with these biological structures. For example, the system could be trained on histological images of tissues, 3D imaging data from organs, or microscopic data from bio-nano structures instead of bacterial cells. The primary challenge lies in ensuring the availability of a sufficiently diverse dataset of images for training the model, similar to the approach used for microorganisms.

The integration of IoBNT technology in the framework can be expanded to capture detailed data from biological systems at different scales. This would allow accurate modeling of larger biological assets while ensuring efficient data collection and transmission. For complex systems like organs or tissues, where interactions are more intricate than with microorganisms, additional pattern recognition layers, such as temporal or 3D spatial patterning, could be incorporated to process time-series or volumetric data. The framework's key strength lies in its flexibility, meaning that with a well-structured dataset for training, it can adapt to various biological assets beyond microorganisms. This adaptability supports applications in biotechnology and digital health.

5.2. Implementation challenges

During the implementation of the framework, a variety of practical challenges were encountered, which significantly impacted its deployment within a laboratory environment. From hardware limitations to data privacy, each presented unique adjustments to make the framework feasible. This section highlights these key challenges and how we addressed them, along with considerations for future improvements. Practical use of IoBNT required adapting our setup to specific hardware needs. One main issue was sourcing IoBNT sensors with the resolution necessary for capturing nano-scale biological data, as many existing lab sensors do not meet this precision. These specialized sensors required more processing power to run MobileNetV2 locally, pushing the limits of the initial devices. Additionally, the continuous data collection increased energy consumption, prompting the need for low-power alternatives to extend operation time without frequent recharging. Future work will focus on energy-efficient hardware optimized for nano-scale applications to support sustainable, long-term use.

Deploying FL on IoBNT devices increased processing demands, particularly for training MobileNetV2 locally. Each device had to complete training independently before syncing with the central server. Although MobileNetV2 is optimized for mobile use, handling larger biological datasets challenged the devices' capabilities. Synchronization delays caused additional latency in data aggregation. To mitigate this, model complexity was reduced where possible, and the communication protocol was optimized. Using lightweight edge hardware, such as TPUs, could further lower latency and enable real-time processing. Data privacy was a key concern, as each IoBNT device handled sensitive biological data. The decentralized FL architecture ensured data remained on local devices, reducing exposure risks. However, securing model aggregation on the central server was crucial, as aggregated updates might reveal indirect data details. To address this, encrypted data transfers were implemented, regulatory standards were followed, and personnel were trained in privacy protocols to protect the framework. Future implementations could integrate additional privacy-preserving methods, such as differential privacy, to enhance security.

Initial testing conducted in controlled laboratory settings revealed certain validation challenges. Consistent data quality from IoBNT sensors was essential for achieving high classification accuracy; however, real-world conditions introduced significant variability. Pilot tests enabled the identification and resolution of initial issues related to model consistency, yet scaling up the framework underscored the necessity for regular recalibration to sustain optimal performance. Continued validation in various lab environments will provide more robust insights into real-world applicability. Scaling the IoBNT-FL framework added practical considerations, particularly as the number of devices and data volumes increased. Coordinating device synchronization and maintenance, such as software updates and recalibrations, became more complex. Planning for operational costs and implementing automated monitoring tools for proactive maintenance helped address these needs. Future implementations could benefit from modular hardware to ease scaling, as well as advancements in sensor technology and edge AI to improve efficiency.

5.3. The framework's importance

The framework proposed in this study represents a fundamental shift in how biotechnological processes can be managed and optimized, with profound implications for several industries. In biotechnology, pharmaceuticals, and healthcare sectors, the DT framework can offer a robust solution for real-time monitoring, simulation, and optimization of biological systems. Specifically, the framework addresses a persistent challenge in biomanufacturing, where ensuring the reliability and accuracy of production processes is paramount. By facilitating the development of real-time DTs for microorganisms and biological systems, the proposed framework significantly enhances the capacity of industries to predict system behavior, diagnose issues, and optimize workflows, thereby reducing the reliance on extensive physical trials. For instance, in pharmaceutical manufacturing, where precision is paramount, this integration can allow for predictive modeling of drug interactions, optimizing dosages, and refining production processes with unprecedented accuracy. The ability to fine-tune these processes without halting production lines not only improves productivity but can also ensure higher quality control, potentially reducing costs and time to market.

Furthermore, the framework's decentralized structure can allow for greater scalability, which is essential for industries with distributed manufacturing operations or research facilities. By utilizing FL, industries can train machine learning models collaboratively across multiple facilities without needing to centralize sensitive biological data, thereby ensuring privacy and compliance with data security regulations, such as the GDPR in Europe and HIPAA in the United States. This is particularly relevant for industries managing vast quantities of sensitive healthcare data, where security and privacy are of utmost concern. By enabling real-time modeling of patient-specific biological systems, the framework can offer unprecedented opportunities for personalized treatment plans that adapt in real-time based on patient responses. This can mark a significant advancement in the delivery of healthcare, contributing to more effective, efficient, and tailored treatments.

The proposed DT framework expands the existing research on DT and Federated Learning, particularly in biotechnology and healthcare. While most DT studies focus on engineering and industrial applications, fewer have explored the challenges of biological systems. Integrating IoBNT into the DT framework introduces a new perspective to the literature. Although IoT applications are widely studied across various fields, IoBNT specifically addresses biological systems at nano and micro scales, an area that remains largely unexplored. Additionally, incorporating FL into this framework is a significant contribution, especially given the increasing focus on decentralized ML in medical and healthcare research. While existing studies on FL in healthcare predominantly focus on clinical data, this work extends those studies by applying FL to biological data generated by IoBNT systems. This approach not only addresses critical issues of privacy and security but also enhances the scalability of DTs within the domain of biotechnology. This work also contributes to the literature on bandwidth optimization in distributed networks, an important consideration in industries handling large datasets. By demonstrating how FL can drastically reduce the bandwidth required for data transmission between laboratories and hospitals, the framework can offer a significant improvement over traditional centralized models, which can be bandwidth-intensive and difficult to scale.

From a government and regulatory perspective, this framework can address several key challenges in biotechnology and healthcare, particularly around data privacy, security, and compliance. Governments worldwide are increasingly focusing on the need for secure and privacy-compliant data handling systems, particularly in sectors like healthcare, where data breaches can have serious consequences. The decentralized architecture of the proposed framework, which utilizes FL to allow data to remain local while still enabling collaborative learning, aligns with the growing regulatory emphasis on privacy-preserving technologies. This framework can serve as a valuable tool for governments and public health agencies in pandemic preparedness and response. Real-time DT of biological systems can improve disease monitoring, allowing public health authorities to act more quickly and accurately. For instance, during the COVID-19 pandemic, real-time simulation of disease transmission and modeling the impact of different treatment strategies would have been highly beneficial.

Moreover, this framework can aid governments in managing healthcare infrastructure more efficiently. The ability to monitor and optimize the performance of biological systems in real-time can lead to more efficient use of medical resources, such as optimizing drug manufacturing processes or personalizing medical treatments. This aligns with governmental goals of reducing healthcare costs while improving patient outcomes, making the proposed framework a valuable asset for healthcare policymakers. Finally, the framework's focus on integrating IoBNT with DTs offers significant potential for environmental monitoring, a key concern for governments aiming to combat climate change and environmental degradation. By facilitating real-time monitoring of ecosystems at the nano and micro levels, this technology allows governments to track biodiversity changes, monitor pollution levels, and predict the real-time impact of environmental policies. This approach is in alignment with global sustainability objectives, as it provides a robust mechanism to ensure that policy interventions achieve their intended outcomes.

5.4. Future directions

Moving forward, future research should focus on further refining the feature extraction capabilities of the model to address the misclassification issues observed with certain bacterial species. Incorporating more sophisticated data augmentation techniques or integrating additional biomarkers into the model may help improve its accuracy for challenging classifications. Additionally, expanding the scope of the study to include more diverse datasets from different laboratories and environments will be essential for further validating the generalizability of the CNN-FL framework. As more data becomes available, it will be interesting to explore how the framework performs in real-world applications, particularly in biomanufacturing and clinical diagnostics. Another important direction for future research is the exploration of advanced FL algorithms, such as personalized FL, which can tailor the model to the specific characteristics of each client's data while still benefiting from collaborative learning. This would be particularly useful in scenarios where there are significant variations between datasets, such as in biotechnology and healthcare.

In addition, as a future research direction, our framework can be extended to significantly enhance efficiency in biomanufacturing within the biotechnology sector. A key focus lies in the development of advanced communication protocols for FL, which are essential for enabling seamless data sharing and integration across decentralized manufacturing units. These protocols will facilitate real-time monitoring and optimization of production processes, thereby minimizing downtime and enhancing overall productivity. Additionally, focusing on improving the scalability of CNNs to handle large-scale, high-dimensional data will allow for more precise and rapid analysis of biomanufacturing operations [15]. Overall, implementing these enhancements will lead to streamlined workflows, improved resource utilization, and higher throughput in biomanufacturing. Furthermore, by targeting these research areas, our framework will contribute to significant advancements in biomanufacturing efficiency, ensuring that biotechnological production processes are more effective, reliable, and capable of meeting the industry's growing demands.

Furthermore, the integration of Bio-Nano Things (BNTs) is essential for the IoBNT-empowered framework, necessitating accurate fabrication and design through synthetic nanotechnology and biology [24,69]. BNTs need to interface with cyber domains, actuate within biological domains, and possess sensing, communication, and data processing capabilities. Hence, energy efficiency, biodegradability, and biocompatibility are critical aspects to address. Besides, enhancing the interface between biological systems and BNTs, exploring sustainable energy sources to improve their reliability and performance, and developing new techniques and materials for BNT fabrication could be future research focuses [17]. In addition, developing macro/nano interfaces, including microfluidic chips and nanofluidic channels, and bio/cyber interfaces, such as biosensors and bioactuators, is crucial [17,69]. Also, exploring advanced technologies and materials for innovative design principles to create more scalable and efficient interface systems, and developing methods to enhance data integration and signal translation between these domains, could be areas for future research [21].

Also, the creation of this pioneering framework, which substantially improves the safety and dependability of DTs across nano and macro scales, represents a central achievement of this study. Furthermore, security and energy efficiency are prominent characteristics of this methodology, offering a versatile and user-oriented platform. As a result, its flexibility enhances its applicability across various domains, including biomanufacturing, healthcare systems, and pharmaceuticals, underscoring its extensive potential impact. Moreover, future research will focus on extending this framework to areas such as personalized environmental monitoring and medicine, capitalizing on its adaptability to achieve broader societal and scientific advancements. Additionally, incorporating IoBNT within the biotechnology sector that relies on DTs constitutes an intriguing yet intricate research area, with numerous promising pathways and unresolved questions warranting further exploration. While molecular docking is a fast and widely used technique, primarily suited for exploring molecular interactions and drug discovery, it may offer complementary insights in future studies related to bacterial classification. In this study, we focused on computer vision techniques to classify bacterial species based on image data, emphasizing computational efficiency and accuracy. Therefore, while theoretical approaches may have relevance in complementary studies, they do not directly align with our current study's objectives and methodology. Future work could explore integrating molecular docking methods to enhance the biological insights of our classification framework.

In addition, several emerging technologies could further enhance the effectiveness of DTs in biotechnology. One promising area is the incorporation of augmented reality (AR), virtual reality (VR), and metaverse technologies into DT frameworks. These technologies would enable researchers and practitioners to visualize and interact with complex biological data in immersive environments, allowing for more intuitive manipulation and exploration of digital models, such as cells or organs. This immersive interaction can facilitate better decision-making and understanding of intricate biological processes. Furthermore, the integration of Web3 technologies can significantly enhance data sharing and collaboration across global research networks by providing a decentralized and secure infrastructure. This would ensure both data integrity and accessibility, which are critical in collaborative scientific efforts. Looking forward, the adoption of newer deep learning algorithms, such as transformer-based models, could improve the accuracy and throughput of DT systems in biotechnology. Additionally, adapting the framework to future communication technologies like 6G and Web 3.0 would further enhance its scalability and data transmission capabilities, expanding its potential applications across the biotechnology industry and beyond.

Integrating Web 3.0 into the DT framework can enhance decentralized and secure data exchange in biotechnology networks. Web 3.0 leverages blockchain technology and decentralized applications (dApps) to ensure privacy and secure management of sensitive biological data. By adopting these technologies, the DT framework can uphold data provenance, immutability, and trust across laboratories and biotechnological workflows. This reduces dependence on centralized authorities while improving transparency, data sharing, and collaboration among biotech organizations and healthcare institutions. Additionally, augmented and virtual reality can enhance user interaction with DT in biotechnology. By incorporating AR and VR, the framework can provide immersive and intuitive visualization of biological processes at molecular or cellular levels.

While 5G technology is currently being rolled out, the potential of 6G in revolutionizing connectivity and data transmission cannot be ignored. With 6G, the DT framework can leverage ultra-fast data speeds, low latency, and massive IoT device connections to support real-time, large-scale biotechnological processes. Implementing 6G technology will allow for the seamless transfer of massive biological data sets, even in environments where billions of nanosensors and IoT devices are working simultaneously. This improvement will allow for better real-time monitoring, analysis, and management of biological entities across laboratories and hospitals, pushing the limits of what is possible with the current DT framework. The use of Web 3.0 combined with AR/VR will not only improve the backend processing but also create a seamless, user-friendly interface. For example, AR can be used to overlay data and insights from DT models onto real-world laboratory environments, helping biotech researchers or healthcare professionals visualize biological behaviors. Simultaneously, Web3-based decentralized networks can make access to DTs more inclusive and user-controlled. Users will have secure, authenticated access to the data they need without interference from intermediaries, enabling more efficient workflows in research and diagnosis.

The biotechnology and healthcare sectors require strict data security and privacy due to the sensitivity of biological data. Web 3.0 can address these challenges through encryption, decentralized identity management, and smart contracts. Integrating blockchain into the DT framework enables secure and transparent data sharing between clients, such as laboratories and hospitals, while ensuring that data ownership and access control remain with the data owners. AI algorithms can optimize bandwidth usage, predict biological behaviors, and dynamically adjust network resources in real time. This reduces the strain on network infrastructure while ensuring critical data is transmitted without delay. Additionally, AI can enhance the accuracy and response time of DT by continuously learning from new data generated within the framework.

6. Conclusions

In this work, we presented a highly efficient DT framework powered by CNN-FL and IoBNT to create bacterial DTs. Our proposed framework offers a robust solution for optimizing bandwidth, reducing error, processing biotechnological data, and digitizing biological assets. Moreover, by integrating IoBNT with deep learning algorithms like FL and CNN, our framework significantly enhances the dependability, reliability, and efficiency of DTs in the biotechnology industry. This approach addresses the challenges of employing DTs at nano and micro scales, making it a highly effective solution for modern biotechnological applications. Thus, these advancements lay a foundation for remarkable improvements in digital health interventions and biotechnological methodologies. Although the framework exhibits significant progress, there remain opportunities for further refinement and enhancement. One area of improvement could involve addressing the limitations of using less diverse datasets, which may affect the model's generalizability. Incorporating more varied data and exploring cutting-edge algorithms, such as transformer-based models, could significantly improve processing efficiency. Moreover, adapting the platform's communication system to integrate with next-generation technologies like 6G and Web 3.0 could boost data transmission capabilities and streamline biotechnological applications. These advancements would ensure that the framework remains both effective and adaptable within the context of a rapidly evolving industry.

CRediT authorship contribution statement

Mohammad (Behdad) Jamshidi: Writing – original draft, Visualization, Methodology, Data curation, Conceptualization. **Dinh Thai Hoang:** Writing – review & editing, Validation, Supervision, Investigation. **Diep N. Nguyen:** Writing – review & editing, Resources, Project administration, Investigation. **Dusit Niyato:** Writing – review & editing, Validation, Investigation. **Majid Ebrahimi Warkiani:** Writing – review & editing, Investigation.

Declaration of competing interest

The authors declare that they have no known competing financial interests or personal relationships that could have appeared to influence the work reported in this paper.

References

[1] S. Khan, A. Alzaabi, T. Ratnarajah, T. Arslan, Novel statistical time series data augmentation and machine learning based classification of unobtrusive respiration data for respiration digital twin model, Comput. Biol. Med. 168 (2024) 107825, http://dx.doi.org/10.1016/j.compbiomed.2023.107825.

[2] A. De Benedictis, N. Mazzocca, A. Somma, C. Strigaro, Digital twins in healthcare: an architectural proposal and its application in a social distancing case study, IEEE J. Biomed. Heal. Informatics 86 (10) (2023) 5143–5154, http://dx.doi.org/10.1109/JBHI.2022.3205506.

[3] M. Alazab, L.U. Khan, S. Koppu, S.P. Ramu, M. Iyapparaja, P. Boobalan, T. Baker, P.K.R. Maddikunta, T.R. Gadekallu, A. Aljuhani, Digital twins for healthcare 4.0-recent advances, architecture, and open challenges, IEEE Consum. Electron. Mag. 12 (6) (2023) 29–37, http://dx.doi.org/10.1109/MCE.2022.3208986.

[4] S. Kim, S. Heo, An agricultural digital twin for mandarins demonstrates the potential for individualized agriculture, Nat. Commun. 15 (1) (2024) 1561, http://dx.doi.org/10.1038/s41467-024-45725-x.

[5] R. Laubenbacher, A. Niarakis, T. Helikar, G. An, B. Shapiro, R.S. Malik-Sheriff, T. Sego, A. Knapp, P. Macklin, J.A. Glazier, Building digital twins of the human immune system: toward a roadmap, NPJ Digit. Med. 5 (1) (2022) 64, http://dx.doi.org/10.1038/s41746-022-00610-z.

[6] Y. Huang, M. Wen, L. Lin, B. Li, Z. Wei, D. Tang, J. Li, W. Duan, W. Guo, Physical-layer counterattack strategies for the internet of bio-nano things with molecular communication, IEEE Internet Things Mag. 6 (2) (2023) 82–87, http://dx.doi.org/10.1109/IOTM.001.2300029.

[7] K. Maksymenko, A.K. Clarke, I. Mendez Guerra, S. Deslauriers-Gauthier, D. Farina, A myoelectric digital twin for fast and realistic modelling in deep learning, Nat. Commun. 14 (1) (2023) 1600, http://dx.doi.org/10.1038/s41467-023-37238-w.

[8] P. Michaux, B. Gaume, Y. Cong, O. Quéméner, Human body numerical simulation: An accurate model for a thigh subjected to a cold treatment, Comput. Biol. Med. 168 (2024) 107689, http://dx.doi.org/10.1016/j.compbiomed.2023.107689.

[9] E. Katsoulakis, Q. Wang, H. Wu, L. Shahriyari, R. Fletcher, J. Liu, L. Achenie, H. Liu, P. Jackson, Y. Xiao, et al., Digital twins for health: a scoping review, NPJ Digit. Med. 7 (1) (2024) 77, http://dx.doi.org/10.1038/s41746-024-01073-0.

[10] E. Behle, J.M. Herold, A.H. Schug, Towards cellular digital twins of in vivo tumors, Biophys. J. 122 (3) (2023) 301a–302a, http://dx.doi.org/10.1016/j.bpj.2022.11.1700.

[11] R.M.C. Portela, C. Varsakelis, A. Richelle, N. Giannelos, J. Pence, S. Dessoy, M. von Stosch, When is an in silico representation a digital twin? A biopharmaceutical industry approach to the digital twin concept, in: C. Herwig, R. Pörtner, J. Möller (Eds.), Digital Twins: Tools and Concepts for Smart Biomanufacturing, Springer International Publishing, Cham, 2021, pp. 35–55, http://dx.doi.org/10.1007/10_2020_138.

[12] M. Sokolov, M. von Stosch, H. Narayanan, F. Feidl, A. Butté, Hybrid modeling—a key enabler towards realizing digital twins in biopharma? Curr. Opin. Chem. Eng. 34 (2021) 100715, http://dx.doi.org/10.1016/j.coche.2021.100715.

[13] A.J. Lopatkin, J.J. Collins, Predictive biology: modelling, understanding and harnessing microbial complexity, Nat. Rev. Microbiol. 18 (9) (2020) 507–520, http://dx.doi.org/10.1038/s41579-020-0372-5.

[14] C. Spahn, E. Gómez-de Mariscal, R.F. Laine, P.M. Pereira, L. von Chamier, M. Conduit, M.G. Pinho, G. Jacquemet, S. Holden, M. Heilemann, et al., DeepBacs for multi-task bacterial image analysis using open-source deep learning approaches, Commun. Biology 5 (1) (2022) 688, http://dx.doi.org/10.1038/s42003-022-03634-z.

[15] C.-S. Ho, N. Jean, C.A. Hogan, L. Blackmon, S.S. Jeffrey, M. Holodniy, N. Banaei, A.A. Saleh, S. Ermon, J. Dionne, Rapid identification of pathogenic bacteria using Raman spectroscopy and deep learning, Nat. Commun. 10 (1) (2019) 4927, http://dx.doi.org/10.1038/s41467-019-12898-9.

[16] A. Hoarfrost, A. Aptekmann, G. Farfañuk, Y. Bromberg, Deep learning of a bacterial and archaeal universal language of life enables transfer learning and illuminates microbial dark matter, Nat. Commun. 13 (1) (2022) 2606, http://dx.doi.org/10.1038/s41467-022-30070-8.

[17] U.A. Chude-Okonkwo, R. Malekian, B.T. Maharaj, Biologically inspired bio-cyber interface architecture and model for internet of bio-nanothings applications, IEEE Trans. Commun. 64 (8) (2016) 3444–3455, http://dx.doi.org/10.1109/TCOMM.2016.2582870.

[18] W.N. Price, I.G. Cohen, Privacy in the age of medical big data, Nature Med. 25 (1) (2019) 37–43, http://dx.doi.org/10.1038/s41591-018-0272-7.

[19] A. Krüger, C. Schäfers, P. Busch, G. Antranikian, Digitalization in microbiology–paving the path to sustainable circular bioeconomy, New Biotechnol. 59 (2020) 88–96, http://dx.doi.org/10.1016/j.nbt.2020.06.004.

[20] G. Nelson, S. Ellis, The history and impact of digitization and digital data mobilization on biodiversity research, Philos. Trans. R. Soc. B 374 (1763) (2019) 20170391, http://dx.doi.org/10.1098/rstb.2017.0391.

[21] A. Signoroni, A. Ferrari, S. Lombardi, M. Savardi, S. Fontana, K. Culbreath, Hierarchical AI enables global interpretation of culture plates in the era of digital microbiology, Nat. Commun. 14 (1) (2023) 6874, http://dx.doi.org/10.1038/s41467-023-42563-1.

[22] IEEE-Standards, IEEE approved draft recommended practice for nanoscale and molecular communication framework, IEEE P1906. 1/ D2. 1, Oct. 2015 (P1906.1/D2.1) (2015) 1–62, https://ieeexplore.ieee.org/document/7294595.

[23] S. Zafar, M. Nazir, A. Sabah, A.D. Jurcut, Securing bio-cyber interface for the internet of bio-nano things using particle swarm optimization and artificial neural networks based parameter profiling, Comput. Biol. Med. 136 (2021) 104707, http://dx.doi.org/10.1016/j.compbiomed.2021.104707.

[24] I.F. Akyildiz, M. Pierobon, S. Balasubramaniam, Y. Koucheryavy, The internet of bio-nano things, IEEE Commun. Mag. 53 (3) (2015) 32–40, http://dx.doi.org/10.1109/MCOM.2015.7060516.

[25] C. Lee, B.-H. Koo, C.-B. Chae, R. Schober, The internet of bio-nano things in blood vessels: System design and prototypes, J. Commun. Networks (2023) http://dx.doi.org/10.23919/JCN.2023.000001.

[26] IEEE-Standards, IEEE standard for information technology - telecommunications and information exchange between systems - local and metropolitan area networks - specific requirements - part 11: Wireless LAN medium access control (MAC) and physical layer (PHY) specifications, IEEE Std 802. 11- 2007 (Revis. IEEE Std 802. 11- 1999) (2007) 1–1076, http://dx.doi.org/10.1109/IEEESTD.2007.373646.

[27] IEEE-Standards, IEEE approved draft recommended practice for routing packets in ieee 802.15.4 dynamically changing wireless networks amendment to fully define use of addressing and route information currently in the standard - amendment a, IEEE P802. 15. 10a/ D03, Novemb. 2018 (35.110 - Networking) (2019) 1–22, https://ieeexplore.ieee.org/servlet/opac?punumber=8559696.

[28] A. Pandi, D. Adam, A. Zare, V.T. Trinh, S.L. Schaefer, M. Burt, B. Klabunde, E. Bobkova, M. Kushwaha, Y. Foroughijabbari, et al., Cell-free biosynthesis combined with deep learning accelerates de novo-development of antimicrobial peptides, Nat. Commun. 14 (1) (2023) 7197, http://dx.doi.org/10.1038/s41467-023-42434-9.

[29] T.T. Van Tran, H. Tayara, K.T. Chong, AMPred-CNN: Ames mutagenicity prediction model based on convolutional neural networks, Comput. Biol. Med. 176 (2024) 108560, http://dx.doi.org/10.1016/j.compbiomed.2024.108560.

[30] Q. Han, X. Qian, H. Xu, K. Wu, L. Meng, Z. Qiu, T. Weng, B. Zhou, X. Gao, DM-CNN: Dynamic multi-scale convolutional neural network with uncertainty quantification for medical image classification, Comput. Biol. Med. 168 (2024) 107758, http://dx.doi.org/10.1016/j.compbiomed.2023.107758.

[31] N. Rieke, J. Hancox, W. Li, F. Milletari, H.R. Roth, S. Albarqouni, S. Bakas, M.N. Galtier, B.A. Landman, K. Maier-Hein, et al., The future of digital health with federated learning, NPJ Digit. Med. 3 (1) (2020) 1–7, http://dx.doi.org/10.1038/s41746-020-00323-1.

[32] W.Y.B. Lim, N.C. Luong, D.T. Hoang, Y. Jiao, Y.-C. Liang, Q. Yang, D. Niyato, C. Miao, Federated learning in mobile edge networks: A comprehensive survey, IEEE Commun. Surv. & Tutorials 22 (3) (2020) 2031–2063, http://dx.doi.org/10.1109/COMST.2020.2986024.

[33] A. Almodóvar, J. Parras, S. Zazo, Propensity weighted federated learning for treatment effect estimation in distributed imbalanced environments, Comput. Biol. Med. 178 (2024) 108779, http://dx.doi.org/10.1016/j.compbiomed.2024.108779.

[34] D. Huang, X. Ye, T. Sakurai, Multi-party collaborative drug discovery via federated learning, Comput. Biol. Med. 171 (2024) 108181, http://dx.doi.org/10.1016/j.compbiomed.2024.108181.

[35] S. Maedera, T. Mizuno, H. Kusuhara, Investigation of latent representation of toxicopathological images extracted by CNN model for understanding compound properties in vivo, Comput. Biol. Med. 168 (2024) 107748, http://dx.doi.org/10.1016/j.compbiomed.2023.107748.

[36] R. Kumar, C.M. Bernard, A. Ullah, R.U. Khan, J. Kumar, D.K. Kulevome, R. Yunbo, S. Zeng, Privacy-preserving blockchain-based federated learning for brain tumor segmentation, Comput. Biol. Med. (2024) 108646, http://dx.doi.org/10.1016/j.compbiomed.2024.108646.

[37] C. Ding, O. Yang, M. Ierapetritou, Towards digital twin for biopharmaceutical processes: Concept and progress, in: R. Pörtner (Ed.), Biopharmaceutical Manufacturing: Progress, Trends and Challenges, Springer International Publishing, Cham, 2023, pp. 179–211, http://dx.doi.org/10.1007/978-3-031-45669-5_6.

[38] S.-Y. Park, C.-H. Park, D.-H. Choi, J.K. Hong, D.-Y. Lee, Bioprocess digital twins of mammalian cell culture for advanced biomanufacturing, Curr. Opin. Chem. Eng. 33 (2021) 100702, http://dx.doi.org/10.1016/j.coche.2021.100702.

[39] A. Schmidt, H. Helgers, L.J. Lohmann, F. Vetter, A. Juckers, M. Mouellef, S. Zobel-Roos, J. Strube, Process analytical technology as key-enabler for digital twins in continuous biomanufacturing, J. Chem. Technol. Biotechnol. 97 (9) (2022) 2336–2346, http://dx.doi.org/10.1002/jctb.7008.

[40] A. Shoshi, Y. Xia, A. Fieschi, T. Ackermann, P. Reimann, M. Weyrich, B. Mitschang, T. Bauernhansl, R. Miehe, A flexible digital twin framework for ATMP production–towards an efficient CAR t cell manufacturing, Procedia CIRP 125 (2024) 124–129, http://dx.doi.org/10.1016/j.procir.2024.08.022.

[41] B. Mahanty, Hybrid modeling in bioprocess dynamics: Structural variabilities, implementation strategies, and practical challenges, Biotechnol. Bioeng. 120 (8) (2023) 2072–2091, http://dx.doi.org/10.1002/bit.28503.

[42] L.G. Wang, R. Ge, X. Chen, R. Zhou, H.-M. Chen, Multiscale digital twin for particle breakage in milling: From nanoindentation to population balance model, Powder Technol. 386 (2021) 247–261, http://dx.doi.org/10.1016/j.powtec.2021.03.005.

[43] M. Wieczorowski, D. Kucharski, P. Sniatala, P. Pawlus, G. Krolczyk, B. Gapinski, A novel approach to using artificial intelligence in coordinate metrology including nano scale, Measurement 217 (2023) 113051, http://dx.doi.org/10.1016/j.measurement.2023.113051.

[44] S.M. Abd El-atty, P. Vijayakumar, O. Alfarraj, M. Karuppiah, F. Shawki, Bioinspired molecular communications system for targeted drug delivery with IoBNT-based sustainable biocyber interface, Comput. Electr. Eng. 118 (2024) 109452, http://dx.doi.org/10.1016/j.compeleceng.2024.109452.

[45] I.F. Akyildiz, M. Ghovanloo, U. Guler, T. Ozkaya-Ahmadov, A.F. Sarioglu, B.D. Unluturk, PANACEA: An internet of bio-nanothings application for early detection and mitigation of infectious diseases, IEEE Access 8 (2020) 140512–140523, http://dx.doi.org/10.1109/ACCESS.2020.3012139.

[46] L.U. Khan, E. Mustafa, J. Shuja, F. Rehman, K. Bilal, Z. Han, C.S. Hong, Federated learning for digital twin-based vehicular networks: Architecture and challenges, IEEE Wirel. Commun. (2023) http://dx.doi.org/10.1109/MWC.012.2200373.

[47] S.P. Ramu, P. Boopalan, Q.-V. Pham, P.K. Reddy, Federated learning enabled digital twins for smart cities: Concepts, recent advances, and future directions, Sustain. Cities Soc. (ISSN: 2210-6707) 79 (2022) 103663, http://dx.doi.org/10.1016/j.scs.2021.103663.

[48] W. Sun, S. Lei, L. Wang, Z. Liu, Y. Zhang, Adaptive federated learning and digital twin for industrial internet of things, IEEE Trans. Ind. Informatics 17 (8) (2020) 5605–5614, http://dx.doi.org/10.1109/TII.2020.3034674.

[49] Y. Lu, X. Huang, K. Zhang, S. Maharjan, Y. Zhang, Low-latency federated learning and blockchain for edge association in digital twin empowered 6G networks, IEEE Trans. Ind. Informatics 17 (7) (2020) 5098–5107, http://dx.doi.org/10.1109/TII.2020.3017668.

[50] A.A. Movassagh, J.A. Alzubi, M. Gheisari, M. Rahimi, S. Mohan, A.A. Abbasi, N. Nabipour, Artificial neural networks training algorithm integrating invasive weed optimization with differential evolutionary model, J. Ambient. Intell. Humaniz. Comput. (2023) 1–9, http://dx.doi.org/10.1007/s12652-020-02623-6.

[51] R. Kala, M.P.A. Punitha, P. Banupriya, B. Veerasamy, B. Bharathi, J.A.A. Alzubi, A deep neural network for image classification using mixed analog and digital infrastructure, in: International Conference on Emergent Converging Technologies and Biomedical Systems, Springer, 2023, pp. 657–665, http://dx.doi.org/10.1007/978-981-99-8646-0_51.

[52] U. Kose, O. Deperlioglu, J. Alzubi, B. Patrut, Deep learning for medical decision support systems, Studies in Computational Intelligence, vol. 909, Springer, 2021, http://dx.doi.org/10.1007/978-981-15-6325-6.

[53] J.A. Alzubi, R. Jain, P. Nagrath, S. Satapathy, S. Taneja, P. Gupta, Deep image captioning using an ensemble of CNN and LSTM based deep neural networks, J. Intell. Fuzzy Systems 40 (4) (2021) 5761–5769, http://dx.doi.org/10.3233/JIFS-189415.

[54] M. Islam, M.T. Reza, M. Kaosar, M.Z. Parvez, Effectiveness of federated learning and CNN ensemble architectures for identifying brain tumors using MRI images, Neural Process. Lett. 55 (4) (2023) 3779–3809, http://dx.doi.org/10.1007/s11063-022-11014-1.

[55] A. Lakhan, M.A. Mohammed, K.H. Abdulkareem, H. Hamouda, S. Alyahya, Autism spectrum disorder detection framework for children based on federated learning integrated CNN-LSTM, Comput. Biol. Med. 166 (2023) 107539, http://dx.doi.org/10.1016/j.compbiomed.2023.107539.

[56] Y.N. Tan, V.P. Tinh, P.D. Lam, N.H. Nam, T.A. Khoa, A transfer learning approach to breast cancer classification in a federated learning framework, IEEe Access 11 (2023) 27462–27476, http://dx.doi.org/10.1109/ACCESS.2023.3257562.

[57] W. Yang, W. Xiang, Y. Yang, P. Cheng, Optimizing federated learning with deep reinforcement learning for digital twin empowered industrial IoT, IEEE Trans. Ind. Informatics 19 (2) (2022) 1884–1893, http://dx.doi.org/10.1109/TII.2022.3183465.

[58] R. Eftimie, A. Mavrodin, S.P. Bordas, From digital control to digital twins in medicine: A brief review and future perspectives, Adv. Appl. Mech. 56 (2023) 323–368, http://dx.doi.org/10.1016/bs.aams.2022.09.001.

[59] A. Ferrari, K. Willcox, Digital twins in mechanical and aerospace engineering, Nat. Comput. Sci. 4 (3) (2024) 178–183, http://dx.doi.org/10.1038/s43588-024-00613-8.

[60] M.W. Grieves, Digital twins: past, present, and future, in: The Digital Twin, Springer, 2023, pp. 97–121, http://dx.doi.org/10.1007/978-3-031-21343-4_4.

[61] Z. Li, X. Xu, X. Cao, W. Liu, Y. Zhang, D. Chen, H. Dai, Integrated CNN and federated learning for COVID-19 detection on chest X-ray images, IEEE/ACM Trans. Comput. Biology Bioinform. (2022) http://dx.doi.org/10.1109/TCBB.2022.3184319.

[62] M. Canzoneri, A. De Luca, J. Harttung, Digital twins: A general overview of the biopharma industry, in: Advances in Biochemical Engineering/Biotechnology, Springer, 2021, pp. 167–184, http://dx.doi.org/10.1007/10_2020_157.

[63] C. Herwig, R. Pörtner, J. Möller, Digital Twins: Tools and Concepts for Smart Biomanufacturing, Springer, 2021, http://dx.doi.org/10.1007/978-3-030-71660-8.

[64] C.L. Gargalo, S.C. de las Heras, M.N. Jones, I. Udugama, S.S. Mansouri, U. Krühne, K.V. Gernaey, Towards the development of digital twins for the bio-manufacturing industry, in: C. Herwig, R. Pörtner, J. Möller (Eds.), Digital Twins: Tools and Concepts for Smart Biomanufacturing, Springer International Publishing, Cham, 2021, pp. 1–34, http://dx.doi.org/10.1007/10_2020_142.

[65] K. Gkouskou, I. Vlastos, P. Karkalousos, D. Chaniotis, D. Sanoudou, A.G. Eliopoulos, The “virtual digital twins” concept in precision nutrition, Adv. Nutr. 11 (6) (2020) 1405–1413, http://dx.doi.org/10.1093/advances/nmaa089.

[66] F.J.M. Shamrat, S. Azam, A. Karim, K. Ahmed, F.M. Bui, F. De Boer, High-precision multiclass classification of lung disease through customized MobileNetV2 from chest X-ray images, Comput. Biol. Med. 155 (2023) 106646, http://dx.doi.org/10.1016/j.compbiomed.2023.106646.

[67] Q. Zhou, G. Zheng, FedContrast-GPA: Heterogeneous federated optimization via local contrastive learning and global process-aware aggregation, in: International Conference on Medical Image Computing and Computer-Assisted Intervention, Springer, 2023, pp. 660–670, http://dx.doi.org/10.1007/978-3-031-43895-0_62.

[68] D.J. Beutel, T. Topal, A. Mathur, X. Qiu, J. Fernandez-Marques, Y. Gao, L. Sani, K.H. Li, T. Parcollet, P.P.B. de Gusmão, et al., Flower: A friendly federated learning research framework, 2020, http://dx.doi.org/10.48550/arXiv.2007.14390, arXiv preprint arXiv:2007.14390.

[69] Y. Tang, Y. Huang, C.-B. Chae, W. Duan, M. Wen, L.-L. Yang, Molecular-type permutation shift keying in molecular MIMO communications for iobnt, IEEE Internet Things J. 8 (21) (2021) 16023–16034, http://dx.doi.org/10.1109/JIOT.2021.3051405.

[70] R. Yacouby, D. Axman, Probabilistic extension of precision, recall, and f1 score for more thorough evaluation of classification models, in: Proceedings of the First Workshop on Evaluation and Comparison of NLP Systems, Association for Computational Linguistics, 2020, pp. 79–91, http://dx.doi.org/10.18653/v1/2020.eval4nlp-1.9.

[71] M.B. Jamshidi, S. Sargolzaei, S. Foorginezhad, O. Moztarzadeh, Metaverse and microorganism digital twins: A deep transfer learning approach, Appl. Soft Comput. 147 (2023) 110798, http://dx.doi.org/10.1016/j.asoc.2023.110798.

[72] M. Sandler, A. Howard, M. Zhu, A. Zhmoginov, L.-C. Chen, Mobilenetv2: Inverted residuals and linear bottlenecks, in: Proceedings of the IEEE Conference on Computer Vision and Pattern Recognition, 2018, pp. 4510–4520, http://dx.doi.org/10.48550/arXiv.1801.04381.